

UTRECHT UNIVERSITY

MSC MATHEMATICAL SCIENCES

MASTER THESIS

**Smile Risk in Expected Shortfall
Estimation for Interest Rate Options**

Author:

KAY BOGERD

Supervisors:

DR. GERGELY CSAPÓ (RABOBANK)

LEONIE VAN DEN BERGE, MSC (RABOBANK)

PROF. DR. ROBERTO FERNÁNDEZ (UU)

DR. KARMA DAJANI (UU)

November 6, 2015



Utrecht University
Faculty of Science
Master Mathematical Sciences
Princetonplein 5
3584 CC Utrecht



Rabobank

Rabobank Nederland
Risk Management
Model Validation
P.O. Box 17100
3500 HG Utrecht

Abstract

This thesis aims to further develop historical simulation methods and focuses on the market risk of interest rate options in the presence of negative interest rates. To accommodate these negative interest rates, a typical solution is to shift the interest rates to lift them into positive territory, where the conventional pricing functions can be used again. We derive an adaptation of the SABR formula that allows us to compare implied volatilities obtained with different shift parameters. Using this method we are able to find risk factors that can be used to perform a historical simulation without the need for numerical calibration algorithms. Furthermore, we investigate if the currently applied methods can be improved by incorporating additional risk factors that can account for changes in the shape of the volatility smile.

Our results show that the studied historical simulation methods can provide accurate prediction of both the value at risk and the expected shortfall. However, we do not find strong evidence to support that modeling volatility smile changes improves the accuracy of a historical simulation.

Preface

This thesis was written in partial fulfillment of the requirements for the degree of Master of Science in Mathematical Sciences at Utrecht University. Before I started this thesis, I was interested in a research project that would allow me to experience the practical aspects of mathematics in finance. Rabobank gave me the opportunity to conduct research as an intern of the Model Validation team. In my time there, I had the pleasure of being included in a group of kind and competent experts. The interesting conversations and discussions allowed me to further develop my skills and contributed to a truly great experience.

I take this opportunity to thank everyone who has helped me during my research. First of all, I would like to express my gratitude to my supervisors from the Rabobank, Gergely Csapó and Leonie van den Berge, their continued support and guidance have contributed greatly to this thesis and my experience at the Rabobank. I would also like to thank my supervisors from Utrecht University, Roberto Fernández and Karma Dajani. Furthermore, the many discussions I had with Misha van Beek and Lech Grzelak have given me valuable insights which contributed significantly to this thesis, and for this I am grateful. I would also like to thank my fellow student Wouter van Krieken, for proofreading this thesis and who gave a lot of useful feedback. Lastly, I would like to thank my partner and parents for their support throughout my study and especially in finishing this research project.

Kay Bogerd
November 6, 2015

Contents

Abstract	v
Preface	vii
1 Introduction	1
1.1 Research Problem	2
1.2 Delimitations	2
1.3 Thesis Structure	2
2 Pricing Interest Rate Instruments	5
2.1 Interest Rates	5
2.1.1 Libor Rates	6
2.1.2 Swap Rates	8
2.2 Measures	9
2.2.1 T -Forward Measure	9
2.2.2 Swap Measure	10
2.3 Options	10
2.3.1 Caps and Floors	11
2.3.2 Swaptions	13
2.4 Option Pricing	14
2.4.1 Black's Model	14
2.4.1.1 Shifted Black's Model	16
2.4.2 Bachelier's Model	17
2.4.3 SABR Model	19
2.4.3.1 Shifted SABR Model	24
2.5 Bootstrapping Market Data	27
3 Risk Measurement	31
3.1 Risk Measures	31
3.1.1 Monetary and Coherent Risk Measures	32
3.1.2 Value at Risk	33
3.1.3 Expected Shortfall	34

3.2	Estimating Profit and Loss	36
3.2.1	Historical Simulation	36
3.2.2	Value at Risk Estimation	38
3.2.3	Expected Shortfall Estimation	39
3.3	Backtesting	39
3.3.1	Backtesting Value at Risk	39
3.3.1.1	Unconditional Coverage	40
3.3.1.2	Independence	41
3.3.2	Backtesting Expected Shortfall	42
3.3.2.1	Unconditional Coverage	44
3.3.2.2	Independence	45
4	Risk Measurement for Interest Rate Options	47
4.1	Interest Rate Shocks	47
4.2	Implied Volatility Shocks	48
4.2.1	Using Black's Model	49
4.2.1.1	Malz's Method	49
4.2.1.2	Level, Slope, and Curvature Method	50
4.2.2	Using Bachelier's Model	53
4.2.2.1	Malz's Method	53
4.2.2.2	Level, Slope, and Curvature Method	54
4.2.3	Using the SABR Model	57
4.3	Summary	58
5	Empirical Study and Results	61
5.1	Market Data	61
5.2	Test Portfolio	62
5.3	Backtests	63
5.3.1	Effect of s_B in Black's Model Based Methods	64
5.3.2	Effect of β and s in SABR Model Based Methods	66
5.3.3	Accuracy of Each Method	67
6	Conclusion	71
	References	73

List of Figures

2.1	Typical shapes that arise when the implied volatility is plotted against the strike for options with the same expiry.	20
2.2	Effect of the SABR parameters on the implied volatility smile.	23
2.3	Prices in basis points when using different values for the shift s_B in Theorem 2.28 with constant SABR parameters.	27
2.4	Bootstrapped discount curve, forward curve and forward swap curve.	29
3.1	Example of how to calculate shocks from risk factor values.	37
4.1	Calibration of the SABR model with different values β and s , using three shifted Black implied volatilities.	50
4.2	Recovering SABR parameters from the level, slope, and curvature.	53
4.3	Calibration of the SABR model with different values β and s , using three normal implied volatilities.	54
4.4	Recovering SABR parameters from the level, slope, and curvature.	56
5.1	Forward swap rates for different combinations of maturity \times tenor.	62
5.2	Time series of the realized profit and loss compared to the value at risk and expected shortfall estimates.	69

List of Tables

4.1	Analytic recalibration of the shifted Black implied volatility smile. . .	52
4.2	Analytic recalibration of the normal implied volatility smile.	56
5.1	Value at risk backtest results of the Black's model based methods. . .	65
5.2	Expected shortfall backtest results of the Black's model based methods.	65
5.3	Value at risk backtest results of the SABR model based methods. . .	66
5.4	Expected shortfall backtest results of the SABR model based methods.	67
5.5	Value at risk backtest results of each method.	68
5.6	Expected shortfall backtest results of each method.	68

Chapter 1

Introduction

Risk management is an essential part of running a financial institution. After a period of extreme stress in the financial sector, such as during the European debt crisis, risk management got renewed focus. Risk measurement is an important aspect of risk management, because the risk measures are used both for the assessment of internal trading risk limits and for the calculation of regulatory capital requirements. Therefore, developing accurate yet practical methods for risk measurement is imperative to any organization that participates in the financial markets.

As a result of the European debt crisis, interest rates are, and have been, at an historically low level. Recently, even the Euribor, a key reference rate, has fallen into negative territory for the first time since its inception. Because such a scenario was previously considered impossible, many of the pricing models applied in finance work under the assumption that interest rates are positive. In particular, the market for interest rate options has changed significantly with the advent of pricing models allowing for negative interest rates. Since many risk measurement methods depend, either explicitly or implicitly, on such pricing models, risk management cannot stay behind and needs to update its methodologies.

From a regulatory perspective, institutions are required to calculate their capital requirements based on their risk measures. The regulator attempts to quantify the risk exposure in this manner, ensuring that potential future losses can be covered by the retained capital. Since the Basel Committee on Banking Supervision obligated banks to adopt the value at risk as risk measure for market risk, it has become the most used risk measure in the financial industry. The widespread use of value at risk has led to quite some criticism as it does not account for shortfall risk, which could encourage more risk taking and higher losses. The deficiencies of value at risk have eventually led to the decision to replace value at risk with a new risk measure, namely the expected shortfall. While solving many of the problems associated with value at risk, the expected shortfall is a more complex risk measure, and more advanced methods might be needed to estimate it accurately.

1.1 Research Problem

The main purpose of this thesis is to determine the accuracy of the historical simulation method in estimating the value at risk and the expected shortfall. In particular, we will investigate which risk factors perform best on portfolios with interest rate options. Because interbank interest rates have become negative in recent months, this task requires the development of novel methods capable of estimating the value at risk and the expected shortfall, even in markets with negative interest rates.

The second, and perhaps more interesting question, is whether modeling changes in the shape of the volatility smile by additional risk factors can significantly increase the estimation accuracy. Since the expected shortfall requires more accurate estimation of tail events, we are specifically interested in determining if the addition of more risk factors can improve the accuracy for the expected shortfall. To this end, we need to derive risk factors which model the shape of the volatility and can be used efficiently within a historical simulation. This is of practical importance, since computationally inefficient methods generally become infeasible when used on large portfolios, as is the case for Rabobank.

1.2 Delimitations

This thesis will only focus on the estimation of risk measures using the historical simulation method. As such, this report tries to determine which risk factors are the most representative for a portfolio consisting of interest rate options and it is not meant to compare historical simulation to other methods.

Another limitation is associated with the implementation of the backtests. Since the estimates are computed for hypothetical positions opened and closed on a daily interval, which is a drastic simplification compared to real life positions. Furthermore, the position pricing is imperfect as a decline in time to maturity is ignored in the scenarios generated by the historical simulation. However, since our estimates are based on one day ahead forecasts, these effect will be negligible, since the smallest maturity used in this thesis is one year.

1.3 Thesis Structure

The remainder of this report is structured as follows. In Chapter 2, we develop the necessary background theory for interest rate options. We specifically focus on the theory needed to price these options, and present multiple pricing methods, which are required for later parts of this report. Chapter 3 continues with the introduction

of risk measures. We present the historical simulation method used to estimate the risk measures in this thesis and also provide the statistical tools necessary to assess the estimation quality.

Using the background theory, Chapter 4 is used to derive risk factors that can be used in a historical simulation to provide estimates for the value at risk and the expected shortfall of interest rate options, even when the interest rates are negative. In Chapter 5, we apply our methods on recent market data to assess the quality of each method. Chapter 6 reports the conclusions and recommendations of this thesis.

Chapter 2

Pricing Interest Rate Instruments

In this chapter we introduce some basic interest rate instruments and derive their pricing functions. To this end, we will show how these instruments can be related and introduce some important probability measures. The theory in this chapter will then form the basis for the development of the value at risk and expected shortfall models in Chapter 4.

Throughout this thesis we assume an arbitrage free and complete market where non-dividend paying securities are traded continuously inside a finite horizon $[0, T]$. We assume that the prices of these instruments are defined on a probability space $(\Omega, \mathcal{F}, \mathbb{P})$, where Ω is the sample space, \mathcal{F} is a σ -algebra on Ω and \mathbb{P} is a probability measure on the measurable space (Ω, \mathcal{F}) . The information available at time $t \in [0, T]$ is modeled by a filtration $\mathcal{F}_t = \sigma\{W(s), s \in [0, t]\}$ possibly augmented to satisfy the usual conditions, and where W is a m -dimensional Brownian motion.

2.1 Interest Rates

We start this section with the definition of the zero-coupon bond. This is an essential instrument since we can express all interest rates in terms of one, or more, zero-coupon bonds, which in turn allows us to relate various types of interest rates.

Definition 2.1 (Zero-coupon bond). A T -maturity zero-coupon bond is a contract that guarantees the holder one unit of currency to be paid at maturity T . The time t value of this contract is denoted by $P(t, T)$.

Clearly, we should have $P(T, T) = 1$. We also assume that $P(t, T) > 0$, and for technical reasons that will be made clear later, we also require that the function $T \mapsto P(t, T)$ is differentiable.

Another important property of the zero-coupon bond lies in the fact that we can compare cash flows at different dates in the future. If we multiply a time T cash

flow by the zero-coupon bond $P(t, T)$, we get the time t value of this cash flow. This technique is called discounting and we will use it extensively when determining the value of interest rate instruments.

Before we introduce interest rates, we start by adding some structure to time instants and time increments. A tenor structure is a set of real numbers representing all time points of interest for our model.

Definition 2.2 (Tenor structure). A tenor structure $(T_i)_{i \in \{0, \dots, N\}}$ is an increasing sequence of non-negative real numbers, that satisfies

$$0 \leq T_0 < T_1 < \dots < T_N < \infty.$$

Furthermore, the length of the interval between T_i and T_{i+1} is often called the tenor, and is given by

$$\tau_i = T_{i+1} - T_i, \quad \text{for } i \in \{0, \dots, N-1\}.$$

In most cases we take $T_0 = 0$ which should be interpreted as the current time. In most cases we also assume that the tenor is constant, that is $\tau_i = \tau$.

Remark 2.3 (Day count convention). In our definition of a tenor structure all dates are real numbers. In practice, this is not the case and dates are represented as day/month/year. In this case, it might be unclear how to compute the value of the tenors $\tau_i = T_{i+1} - T_i$. To avoid confusion each market has specified a so called day count convention that prescribes how the tenors should be computed.

The most common day count conventions are called Act/360 and Act/365 where τ_i is calculated as the actual number of days between T_i and T_{i+1} divided by 360, and 365, respectively. △

2.1.1 Libor Rates

In general, an interest rate is the amount of money a borrower has to pay to lend money for a specific amount of time expressed as a percentage of the total amount borrowed. In this section we discuss InterBank Offered Rates (Ibor); these are the rates at which large financial institutions are willing to lend money to each other. There are a few different Ibor rates that are fixed by different entities and the fixing entity is differentiated by the prefix. For instance, Libor refers to London InterBank Offered Rate that is fixed by the Intercontinental Exchange and Euribor fixings are determined by the European Banking Federation. Typically Libor serves as a reference for different kinds of products. Although we consider Libor in this section, the same reasoning can be applied to other interbank offered rates.

Consider a large financial institution borrowing one unit of currency at time t that has to be paid back with interest at a later time T_1 . At time t the bank receives one

unit of currency and at time T_1 it has to pay $1 + \tau_0 L(t, T_1)$ units of currency, where $L(t, T_1)$ denotes the time t Libor rate. Discounting the time T_1 cash flow we see that the Libor rate $L(t, T_1)$ has to satisfy the relation

$$P(t, T_1)(1 + \tau_0 L(t, T_1)) = 1. \quad (2.1)$$

Definition 2.4 (Libor rate). The Libor rate with maturity T_1 is the rate that solves equation (2.1) and is given by

$$L(t, T_1) = \frac{1}{T_1 - t} \left(\frac{1}{P(t, T_1)} - 1 \right). \quad (2.2)$$

Instead of borrowing money right now, we might be interested in locking in an interest rate over a period $[T_i, T_{i+1}]$ in the future. This is typically done through a so called forward rate agreement (FRA). A FRA allows the holder to exchange a fixed rate K for a floating rate $L(T_i, T_{i+1})$. So at time T_{i+1} , the holder has to pay $\tau_i K$ and receives $\tau_i L(T_i, T_{i+1})$ units of currency. Therefore, the cash flow of the contract at time T_{i+1} is given by

$$\tau_i(L(T_i, T_{i+1}) - K) = \frac{1}{P(T_i, T_{i+1})} - 1 - \tau_i K. \quad (2.3)$$

Note that, although the cash flow takes place at time T_{i+1} it is already determined at time T_i .

The term $1/P(T_i, T_{i+1})$ in equation (2.3) is worth one unit of currency at time T_i by definition of the zero-coupon bond. Therefore $1/P(T_i, T_{i+1})$ units of currency at time T_{i+1} is worth 1 unit of currency at time T_i , which is equivalent to $P(t, T_i)$ units of currency at time t . By discounting the other terms in equation (2.3), we find that the time t value of the FRA is given by

$$V_{\text{FRA}}^i(t) = P(t, T_i) - P(t, T_{i+1})(1 + \tau_i K). \quad (2.4)$$

This brings us to the definition of forward Libor rates. The forward Libor rate is the Libor rate over a future interval $[T_i, T_{i+1}]$ that is consistent with market prices. Therefore, the forward Libor rate is the value of K in equation (2.4) such that the forward rate agreement has a fair value at time t , so if $V_{\text{FRA}}^i(t) = 0$.

Definition 2.5 (Forward Libor rate). The forward Libor rate for the expiry T_i and maturity T_{i+1} as seen at time t is given by

$$L_i(t) = L(t; T_i, T_{i+1}) = \frac{1}{\tau_i} \left(\frac{P(t, T_i)}{P(t, T_{i+1})} - 1 \right). \quad (2.5)$$

By rewriting equation (2.4), we can express the time t value of a FRA more elegantly in terms of the forward rate

$$V_{\text{FRA}}^i(t) = \tau_i P(t, T_{i+1})(L_i(t) - K). \quad (2.6)$$

2.1.2 Swap Rates

A generalization of the FRA to multiple time intervals is a fixed-for-floating swap (also known as a payer swap). A swap is thus a contract to exchange payments between a fixed rate K and a floating rate $L(T_i, T_{i+1})$ at every instant of a predefined set of times T_{n+1}, \dots, T_m . Note that similar to a FRA the payments are fully determined at times T_i but paid at times T_{i+1} . When the swap starts immediately, i.e. $n = 0$, we call the swap spot starting, otherwise we call it a forward starting swap. The length of the swap $T_m - T_n$ is called the tenor.

Alternatively, when the floating rate is paid and the fixed rate is received, we have a floating-for-fixed swap (also known as a receiver swap). In this section we show how to value a payer swap; a receiver swap can be valued in a similar manner.

The value of a payer swap is simply the sum of multiple FRAs, so by equation (2.6) we find the time t value of a payer swap

$$\begin{aligned} V_{\text{swap}}^{n,m}(t) &= \sum_{i=n}^{m-1} V_{\text{FRA}}^i(t) \\ &= \sum_{i=n}^{m-1} \tau_i P(t, T_{i+1})(L_i(t) - K) \\ &= P(t, T_n) - P(t, T_m) - \sum_{i=n}^{m-1} \tau_i P(t, T_{i+1})K. \end{aligned} \quad (2.7)$$

Similar to forward rates, we can define swap rates. The swap rate is the value for K in equation (2.7) such that the swap has fair value, that is $V_{\text{swap}}^{n,m}(t) = 0$.

Definition 2.6 (Swap Rate). The swap rate $S_{n,m}(t)$ is given by

$$S_{n,m}(t) = \frac{P(t, T_n) - P(t, T_m)}{A_{n,m}(t)}, \quad (2.8)$$

where $A_{n,m}(t)$ is called the annuity of the swap and is given by

$$A_{n,m}(t) = \sum_{i=n}^{m-1} \tau_i P(t, T_{i+1}). \quad (2.9)$$

Note that by rewriting equation (2.7) we can also express the swap's value in terms

of the swap rate

$$V_{\text{swap}}^{n,m}(t) = A_{n,m}(t)(S_{n,m}(t) - K). \quad (2.10)$$

2.2 Measures

The numeraire is an important concept from the theory of arbitrage free pricing and can be any non-dividend paying asset with positive price process, $N(t) > 0$ for all t . The importance of a numeraire comes from the fundamental theorem of asset pricing. This theorem states that for every numeraire there exists a measure $\mathbb{Q} \sim \mathbb{P}$ that is equivalent to the real-world probability measure \mathbb{P} , such that the time t value of a portfolio $V(t)$ relative to this numeraire is a martingale [9, 10], that is

$$\frac{V(t)}{N(t)} = \mathbb{E}_t^{\mathbb{Q}} \left[\frac{V(T)}{N(T)} \right], \quad (2.11)$$

where $\mathbb{E}_t^{\mathbb{Q}}$ denotes the expectation under \mathbb{Q} conditional on \mathcal{F}_t .

The choice of numeraire can greatly simplify calculations. In this section we introduce some numeraires and their related measures and show why they are particularly useful in an interest rate context.

2.2.1 T -Forward Measure

A zero-coupon bond is a positive non-dividend paying asset and therefore we can use it as a numeraire. The corresponding measure is then called the T -forward measure [12].

Definition 2.7 (T_i -forward measure). The T_i -forward measure \mathbb{Q}^{T_i} is the measure that makes the process $V(t)/P(t, T_i)$ a martingale. That is

$$V(t) = P(t, T_i) \mathbb{E}_t^i \left[\frac{V(T)}{P(T, T_i)} \right] = P(t, T_i) \mathbb{E}_t^i [V(T)], \quad \text{for all } T \leq T_i, \quad (2.12)$$

where $V(t)$ is the time t value of a portfolio and \mathbb{E}_t^i is the expectation under the T_i -forward measure \mathbb{Q}^{T_i} conditional on \mathcal{F}_t .

The reason that the T -forward measure is convenient to work with is that the forward rate is a martingale under this measure.

Lemma 2.8. *The forward rate $L_i(t)$ is a martingale under the T_{i+1} -forward measure $\mathbb{Q}^{T_{i+1}}$. That is*

$$\mathbb{E}_t^{i+1} [L_i(T)] = L_i(t), \quad \text{for all } T \leq T_i. \quad (2.13)$$

Proof. By definition of forward rates and the forward measure we have

$$\mathbb{E}_t^{i+1} [L_i(T)] = \frac{1}{\tau_i} \mathbb{E}_t^{i+1} \left[\frac{P(T, T_i)}{P(T, T_{i+1})} \right] - 1 = \frac{1}{\tau_i} \left(\frac{P(t, T_i)}{P(t, T_{i+1})} - 1 \right) = L_i(t). \quad \square$$

2.2.2 Swap Measure

The annuity of a swap is a linear combination of zero-coupon bonds so it can also be seen as a positive non-dividend-paying asset. Therefore, we can also use the annuity as a numeraire. The martingale measure induced by the annuity numeraire is called the swap measure or annuity measure [15].

Definition 2.9 (Swap measure). The swap measure $\mathbb{Q}^{n,m}$ is the measure that makes the process $V(t)/A_{n,m}(t)$ a martingale. That is

$$V(t) = A_{n,m}(t) \mathbb{E}_t^{n,m} \left[\frac{V(T)}{A_{n,m}(T)} \right], \quad \text{for all } T \leq T_n,$$

where $V(t)$ is the time t value of some portfolio and $\mathbb{E}_t^{n,m}$ is the expectation under the swap measure $\mathbb{Q}^{n,m}$ conditional on \mathcal{F}_t .

The main advantage of working with the swap measure is that the swap rate $S_{n,m}(t)$ is a martingale under this measure.

Lemma 2.10. *The swap rate $S_{n,m}(t)$ is a martingale under the swap measure $\mathbb{Q}^{n,m}$. That is*

$$\mathbb{E}_t^{n,m} [S_{n,m}(T)] = S_{n,m}(t), \quad \text{for all } T \leq T_n.$$

Proof. Define $V(t) = P(t, T_n) - P(t, T_m)$. It then follows by definition of the swap measure that $V(t)/A_{n,m}(t)$ is a martingale under this measure. Therefore, we have

$$\mathbb{E}_t^{n,m} [S_{n,m}(T)] = \mathbb{E}_t^{n,m} \left[\frac{P(T, T_n) - P(T, T_m)}{A_{n,m}(T)} \right] = \frac{P(t, T_n) - P(t, T_m)}{A_{n,m}(t)} = S_{n,m}(t). \quad \square$$

2.3 Options

An option is a contract which gives the holder the right, but not the obligation, to buy or sell an underlying instrument at a specified price at or before a later date. Typically, the pre-agreed price is called the strike and the date is called the options expiry. There are two types of option. A call option gives the holder the right to buy, and a put option gives the holder the right to sell, the underlying instrument

for the strike price at expiry. In this section we only consider European options, this means that the option can only be exercised on, and not before, expiry. We then give two examples of options on interest rates. Caps and floors are options where the underlying instrument is the Libor rate and swaptions have a swap as underlying instrument.

2.3.1 Caps and Floors

A caplet gives the holder the right, but not the obligation, to exchange the Libor rate for some fixed rate. This enables the holder to hedge against rising interest rates. The payoff of a caplet is thus similar to that of a FRA, the difference being that payments are only exchanged when they are beneficial to the caplet holder. Therefore, the cash flow of a caplet with expiry T_i , maturity T_{i+1} and strike rate K is given by

$$\tau_i(L(T_i, T_{i+1}) - K)^+.$$

Note that this payoff is known at expiry T_i and not before. However, the payments are made one time step later at T_{i+1} . The time t value of a caplet can then be obtained by discounting the expected future cash flow.

Definition 2.11 (Caplet value). The time t value of a caplet with expiry T_i , maturity T_{i+1} and strike K is given by

$$V_{\text{caplet}}^i(t) = \tau_i P(t, T_{i+1}) \mathbb{E}_t^{i+1} \left[(L(T_i, T_{i+1}) - K)^+ \right]. \quad (2.14)$$

It is not possible to compute the expectation in equation (2.14) without making additional assumptions on the dynamics of the forward rate $L(T_i, T_{i+1})$. In the next section we show some models that will allow us to calculate the expectation and hence determine the value of a caplet.

Caplets are typically not quoted in the market directly. They are quoted as a portfolio consisting of multiple consecutive caplets, called caps. The expiries of these caplets are then called the reset dates. So a cap for the period $[T_n, T_m]$ has resetting dates T_n, \dots, T_{m-1} . We find its time t value simply by summing the values of each individual caplet.

Definition 2.12 (Cap value). The time t value of a cap with strike K that resets at times T_n, \dots, T_{m-1} is given by

$$V_{\text{cap}}^{n,m}(t) = \sum_{i=n}^{m-1} V_{\text{caplet}}^i(t) = \sum_{i=n}^{m-1} \tau_i P(t, T_{i+1}) \mathbb{E}_t^{i+1} \left[(L(T_i, T_{i+1}) - K)^+ \right]. \quad (2.15)$$

The counterpart of a caplet is a floorlet, allowing the holder to hedge against falling interest rates. The cash flow of a floorlet is given by

$$\tau_i(K - L(T_i, T_{i+1}))^+.$$

Note that similar to a caplet the cash flow of a floorlet is fully determined at time T_i but payments are made at time T_{i+1} . Again, by discounting the expected future cash flows, we find the time t value of a floorlet.

Definition 2.13 (Floorlet value). The time t value of a floorlet with expiry T_i , maturity T_{i+1} and strike K is given by

$$V_{\text{floorlet}}^i(t) = \tau_i P(t, T_{i+1}) \mathbb{E}_t^{i+1} \left[(K - L(T_i, T_{i+1}))^+ \right]. \quad (2.16)$$

Also floorlets are not quoted in the market directly, but sold as a portfolio of multiple consecutive floorlets, called a floor. The value of a floor is determined by the sum of each individual floorlet.

Definition 2.14 (Floor value). The time t value of a floor with strike K and resetting at T_n, \dots, T_{m-1} is given by

$$V_{\text{floor}}^{n,m}(t) = \sum_{i=n}^{m-1} V_{\text{floorlet}}^i(t) = \sum_{i=n}^{m-1} \tau_i P(t, T_{i+1}) \mathbb{E}_t^{i+1} \left[(K - L(T_i, T_{i+1}))^+ \right]. \quad (2.17)$$

A useful relation linking the prices of caps and floors with swaps is given by the following lemma. This lemma is typically referred to as the put-call parity.

Lemma 2.15. *Caps and floors are related to a swap by the relation*

$$V_{\text{cap}}^{n,m}(t) - V_{\text{floor}}^{n,m}(t) = V_{\text{swap}}^{n,m}(t). \quad (2.18)$$

Proof. Consider the cash flows at times T_{i+1} with $i = \{n, \dots, m-1\}$ individually. Then the left hand side of equation (2.18) consists of the cash flow of a caplet and a floorlet, which is given by

$$\tau_i(L(T_i, T_{i+1}) - K)^+ - \tau_i(K - L(T_i, T_{i+1}))^+ = \tau_i(L(T_i, T_{i+1}) - K).$$

This is precisely the cash flow of a forward rate agreement. Since all cash flows are equal, we conclude that the prices are also equal. \square

It is market convention to call a cap or floor at-the-money (ATM) if its strike is equal to the forward swap rate of the underlying swap. So, if we exercised the swap today, it would not make or lose any money. Similarly, if exercising the cap today

would make money, we call it in-the-money (ITM) and if it would lose money, we call it out-of-the-money (OTM). Hence, a cap or floor is ATM when

$$K = S_{n,m}(t) = \frac{P(t, T_n) - P(t, T_m)}{A_{n,m}(t)}.$$

When $K > S_{n,m}(t)$, we say that a cap is out-of-the-money (OTM) and a floor is in-the-money (ITM). Similarly, when $K < S_{n,m}(t)$ a cap is ITM and a floor is OTM.

2.3.2 Swaptions

A swap option, or more commonly known as swaption, is an option giving the right, but not the obligation, to enter an interest rate swap at expiry. Typically, the expiry of the option coincides with the first reset date of the underlying swap, and the length of the swap is called the tenor. Depending on whether the swaption is a call or a put option, we call it a payer swaption or a receiver swaption, respectively. In this section we consider a payer swaption, but a similar reasoning can be applied to receiver swaptions.

By equation (2.10), the time T_n payoff of the swaption, resetting at times T_n, \dots, T_{m-1} and with strike K , is given by

$$A_{n,m}(T_n)(S_{n,m}(T_n) - K)^+.$$

Using the swap measure $\mathbb{Q}^{n,m}$, we can conveniently discount the future expected payoff to get the time t value of a swaption.

Definition 2.16 (Payer swaption value). The time t value of a swaption, with strike K and resetting at T_n, \dots, T_{m-1} , is given by

$$\begin{aligned} V_{\text{swaption}}(t) &= A_{n,m}(t) \mathbb{E}_t^{n,m} \left[A_{n,m}(T_n) \frac{(S_{n,m}(T_n) - K)^+}{A_{n,m}(T_n)} \right] \\ &= A_{n,m}(t) \mathbb{E}_t^{n,m} \left[(S_{n,m}(T_n) - K)^+ \right]. \end{aligned} \quad (2.19)$$

Similar to caps and floors, we call a swaption at-the-money (ATM) if exercising it wouldn't make or lose any money. Similarly, if a swaption that is exercised today would make money, we call it in-the-money (ITM) and if it would lose money, we call it out-of-the-money (OTM). Hence, a payer swaption is ATM when

$$K = S_{n,m}(t) = \frac{P(t, T_n) - P(t, T_m)}{A_{n,m}(t)}.$$

When $K < S_{n,m}(t)$ it is ITM and when $K > S_{n,m}(t)$ it is OTM.

2.4 Option Pricing

In the previous section, we have seen that the forward Libor rate $L_i(t)$ and forward swap rate $S_{n,m}(t)$ are martingales under their corresponding measures. In this section, we let $F(t)$ be either the forward Libor rate or forward swap rate. We assume that we are working in the measure that makes $F(t)$ a martingale and let $N(t)$ be the numeraire corresponding to this measure. So the martingale representation theorem shows that

$$dF(t) = c(t, \dots)dW(t), \quad F(0) = F_0, \quad (2.20)$$

where $W(t)$ is Brownian motion and the coefficient c can be deterministic or random and may depend on any information that can be resolved at time t . Note that the dynamics in equation 2.20 don't have a drift term, since the forward rate is a martingale.

When pricing European options, we concern ourselves with either the evaluation of

$$C(F_0, K, T) = N(0)\mathbb{E}_0 \left[(F(T) - K)^+ \right], \quad (2.21)$$

for European call options or

$$P(F_0, K, T) = N(0)\mathbb{E}_0 \left[(K - F(T))^+ \right], \quad (2.22)$$

for European put options. To evaluate these expectations, we need to make additional assumptions about the coefficient c in equation 2.20. In this section we discuss several models that allow us to compute these expectations.

2.4.1 Black's Model

In 1976, Fischer Black introduced what is now probably the most famous model in financial mathematics [6]. In Black's model, we assume that the coefficient $c(t, \dots) = \sigma_B F(t)$ is deterministic but depends on the current value of the forward rate $F(t)$ and one parameter σ_B called Black's volatility. Therefore, the dynamics of equation 2.20 become

$$dF(t) = \sigma_B F(t)dW(t), \quad F(0) = F_0. \quad (2.23)$$

An application of Itô's lemma [37] shows that

$$d \log(F(t)) = -\frac{1}{2}\sigma_B^2 dt + \sigma_B dW(t), \quad F(0) = F_0. \quad (2.24)$$

Hence, $F(t)$ has a log-normal distribution with location $\log(F_0) - \sigma_B^2 t/2$ and scale $\sigma_B \sqrt{t}$. Because of this, Black's model is sometimes also referred to as the log-normal model. It turns out that when using the dynamics from equation (2.23), we can derive an analytical solution for the price of a European call option in equation (2.21).

Theorem 2.17 (Black's formula). *Let $F(t)$ follow the dynamics from equation (2.23). Then the price of a European call option is given by*

$$\begin{aligned} C_B(F_0, K, T; \sigma_B) &= N(0) \mathbb{E}_0 \left[(F(T) - K)^+ \right] \\ &= N(0) (F_0 \Phi(d_+) - K \Phi(d_-)), \end{aligned} \quad (2.25)$$

where Φ is the standard normal cumulative distribution function and

$$d_{\pm} = \frac{\log(F_0/K) \pm \frac{1}{2} \sigma_B^2 T}{\sigma_B \sqrt{T}}.$$

Proof. $F(T)$ has a log-normal distribution with mean $\bar{\mu} = \log(F_0) - \sigma_B^2 T/2$ and standard deviation $\bar{\sigma} = \sigma_B \sqrt{T}$. Therefore, the expectation in equation (2.25) is

$$\begin{aligned} \mathbb{E}_0 \left[(F(T) - K)^+ \right] &= \mathbb{E}_0 [F(T) - K \mid F(T) > K] \mathbb{P}_0(F(T) > K) \\ &= \mathbb{E}_0 [F(T) \mid F(T) > K] \mathbb{P}_0(F(T) > K) - K \mathbb{P}_0(F(T) > K) \\ &= \exp\left(\bar{\mu} + \frac{1}{2} \bar{\sigma}^2\right) \Phi\left(\frac{\bar{\mu} + \bar{\sigma}^2 - \log(K)}{\bar{\sigma}}\right) - K \Phi\left(\frac{\bar{\mu} - \log(K)}{\bar{\sigma}}\right) \\ &= F_0 \Phi(d_+) - K \Phi(d_-), \end{aligned} \quad (2.26)$$

where the partial expectation is given by [44]

$$\mathbb{E}_0 [F(T) \mid F(T) > K] \mathbb{P}_0(F(T) > K) = \exp\left(\bar{\mu} + \frac{1}{2} \bar{\sigma}^2\right) \Phi\left(\frac{\bar{\mu} + \bar{\sigma}^2 - \log(K)}{\bar{\sigma}}\right).$$

Multiplying equation (2.26) by $N(0)$ proves the result. \square

By following the same steps as in Theorem 2.17, we can derive Black's pricing formula for a European put option from equation (2.22).

Theorem 2.18 (Black's formula). *Let $F(t)$ follow the dynamics from equation (2.23). Then the price of a European put option is given by*

$$\begin{aligned} P_B(F_0, K, T; \sigma_B) &= N(0) \mathbb{E}_0 \left[(F(T) - K)^+ \right] \\ &= N(0) (K \Phi(-d_-) - F_0 \Phi(-d_+)), \end{aligned} \quad (2.27)$$

where Φ and d_{\pm} are as given in Theorem 2.17.

Proof. Follows by a similar argument as Theorem 2.17. \square

Black's model can also be used to quantify the discrepancy between the current forward rate F_0 and the strike of an option K . This discrepancy is typically called the moneyness and for Black's model it is defined as

Definition 2.19 (Log-moneyness). The log-moneyness $M(F_0, K)$ is the logarithmic distance between the forward rate F_0 and the strike K ,

$$M(F_0, K) = \log(K/F_0). \quad (2.28)$$

In Section 2.3 we explained when an option is in-the-money or out-of-the-money. Using Definition 2.19, we can quantify how much a certain options is in-the-money or out-of-the-money. That is, when $M(F_0, K) < 0$, a call option is in-the-money and a put option is out-of-the-money. Similarly, when $M(F_0, K) > 0$, a call option is out-of-the-money and a put option is in-the-money. The case $M(F_0, K) = 0$ occurs when the current forward rate F_0 equals the strike of the option K and is called at-the-money.

2.4.1.1 Shifted Black's Model

When assuming the dynamics of Black's model from equation (2.23), the current forward rate F_0 and strike K must be positive. Recently, interest rates in the eurozone have become negative, indicating that we cannot use Black's model as it is. A frequently used solution is to add a small quantity to both the forward rate and the strike such that they are no longer negative, effectively shifting the distribution of $F(t)$. This class of models is typically referred to as shifted Black's model and has the dynamics

$$dF(t) = \sigma_B^{s_B}(F(t) + s_B)dW(t), \quad F(0) = F_0, \quad (2.29)$$

where s_B is called the shift parameter. A superscript s_B is added to the Black volatility $\sigma_B^{s_B}$ to show that this parameter belongs to the shifted version of Black's model.

Modeling a forward rate with the shifted version of Black's model, it is possible for the forward rate to be in the interval $(-s_B, \infty)$. So by choosing s_B positive, we can effectively allow forward rates to become as negative as we want.

It turns out that we can still use Black's formula from Theorems 2.17 and 2.18 to compute the price of European call and put options.

Theorem 2.20. *Let $F(t)$ follow the dynamics from equation (2.29). Then the price of a European call and put options are respectively given by*

$$C_B(F_0 + s_B, K + s_B, T; \sigma_B^{s_B}) \quad \text{and} \quad P_B(F_0 + s_B, K + s_B, T; \sigma_B^{s_B}), \quad (2.30)$$

where C_B and P_B are Black's formula from Theorem 2.17 and Theorem 2.18.

Proof. When $F(t)$ follows the dynamics of shifted Black's model from equation 2.29, then $X(t) = F(t) + s_B$ follows the dynamics of Black's model from equation 2.23. Hence, the price of a European call option is given by

$$\begin{aligned} N(0)\mathbb{E}_0 \left[(F(T) - K)^+ \right] &= N(0)\mathbb{E}_0 \left[(X(T) - (K + s_B))^+ \right] \\ &= C_B(X(0), K + s_B, T; \sigma_B^s) \\ &= C_B(F_0 + s_B, K + s_B, T; \sigma_B^s). \end{aligned}$$

Similarly, the price of a European put option is given by

$$N(0)\mathbb{E}_0 \left[(K - F(T))^+ \right] = P_B(F_0 + s_B, K + s_B, T; \sigma_B^s). \quad \square$$

Note that for every shift parameter, we effectively have a different model. So, σ_B and σ_B^s will yield different option prices, unless $s_B = 0$ of course.

When using the shifted Black's model, we have to adjust the moneyness accordingly. To this end, we define the shifted log-moneyness as follows

Definition 2.21 (Shifted log-moneyness). The shifted log-moneyness $M(F_0, K)$ is the logarithmic distance between the shifted forward rate $F_0 + s_B$ and the shifted strike $K + s_B$,

$$M(F_0, K) = \log((K + s_B)/(F_0 + s_B)). \quad (2.31)$$

2.4.2 Bachelier's Model

The first model in mathematical finance was developed in 1900 by Louis Bachelier [1]. Although martingale pricing theory did not yet exist in that time, we can formulate his model within this framework.

Instead of assuming a log-normal distribution, Bachelier proposed a model where the forward rates have a normal distribution. This has the benefit that the model can also be applied when the forward rate or strike is negative. Since some interest rates in the eurozone have become negative, this model is gaining popularity in the financial industry. In the framework of martingale pricing theory, Bachelier's model assumes that the coefficient $c(t, \dots) = \sigma_N$ is deterministic and constant. Therefore

the dynamics of equation 2.20 become

$$dF(t) = \sigma_N dW(t), \quad F(0) = F_0. \quad (2.32)$$

This is easy to solve and we see that $F(t) = F(0) + \sigma_N W(t)$. Hence, $F(t)$ has a normal distribution with mean F_0 and standard deviation $\sigma_N \sqrt{t}$. Because of this, Bachelier's model is sometimes also referred to as the normal model and the parameter σ_N is referred to as the normal volatility.

When assuming the dynamics of Bachelier's model from equation (2.32), we can derive an analytical solution for the price of a European call option from equation (2.21).

Theorem 2.22 (Bachelier's formula). *Let $F(t)$ follow the dynamics from equation (2.32). Then the price of a European call option is given by*

$$\begin{aligned} C_N(F_0, K, T; \sigma_N) &= N(0) \mathbb{E}_0 \left[(F(T) - K)^+ \right] \\ &= N(0) \sigma_N \sqrt{T} (d \Phi(d) + \phi(d)), \end{aligned} \quad (2.33)$$

where Φ and ϕ are the standard normal cumulative distribution function and standard normal density function, respectively, and

$$d = \frac{F_0 - K}{\sigma_N \sqrt{T}}.$$

Proof. In Bachelier's model $F(T)$ has a normal distribution with mean F_0 and standard deviation $\sigma_N \sqrt{T}$. Therefore, the expectation in equation (2.33) is

$$\begin{aligned} \mathbb{E}_0 \left[(F(T) - K)^+ \right] &= \mathbb{E}_0 [F(T) - K \mid F(T) > K] \mathbb{P}_0(F(T) > K) \\ &= \mathbb{E}_0 [F(T) \mid F(T) > K] \mathbb{P}_0(F(T) > K) - K \mathbb{P}_0(F(T) > K) \\ &= F_0 \Phi \left(\frac{F_0 - K}{\sigma_N \sqrt{T}} \right) + \sigma_N \sqrt{T} \phi \left(\frac{F_0 - K}{\sigma_N \sqrt{T}} \right) - K \Phi \left(\frac{F_0 - K}{\sigma_N \sqrt{T}} \right) \\ &= \sigma_N \sqrt{T} (d \Phi(d) + \phi(d)), \end{aligned} \quad (2.34)$$

where the conditional expectation is given by [44]

$$\mathbb{E}_0 [F(T) \mid F(T) > K] \mathbb{P}_0(F(T) > K) = F_0 \Phi \left(\frac{F_0 - K}{\sigma_N \sqrt{T}} \right) + \sigma_N \sqrt{T} \phi \left(\frac{F_0 - K}{\sigma_N \sqrt{T}} \right).$$

Multiplying equation (2.34) by $N(0)$ proves the result. \square

By following the same steps as in Theorem 2.22 we can derive the pricing formula for a European put option from equation (2.22).

Theorem 2.23 (Bachelier’s formula). *Let $F(t)$ follow the dynamics from equation (2.32). Then the price of a European put option is given by*

$$\begin{aligned} P_N(F_0, K, T; \sigma_N) &= N(0) \mathbb{E}_0 \left[(K - F(T))^+ \right] \\ &= N(0) \sigma_N \sqrt{T} (-d \Phi(-d) + \phi(-d)). \end{aligned} \quad (2.35)$$

where Φ , ϕ and d are as given in Theorem 2.22.

Proof. Follows by a similar argument as Theorem 2.22. □

Bachelier’s model can also be used to quantify the discrepancy between the current forward rate F_0 and the strike of an option K . This discrepancy is typically called the simple moneyness and is defined as

Definition 2.24 (Simple moneyness). The simple moneyness $M(F_0, K)$ is the distance between the forward rate F_0 and the strike K ,

$$M(F_0, K) = K - F_0. \quad (2.36)$$

An option with moneyness $M(F_0, K) = 0$ is called at-the-money. When $M(F_0, K) < 0$, a call option is called in-the-money and a put option is out-of-the-money. Similarly, when $M(F_0, K) > 0$, a call option is called out-of-the-money and a put option is in-the-money.

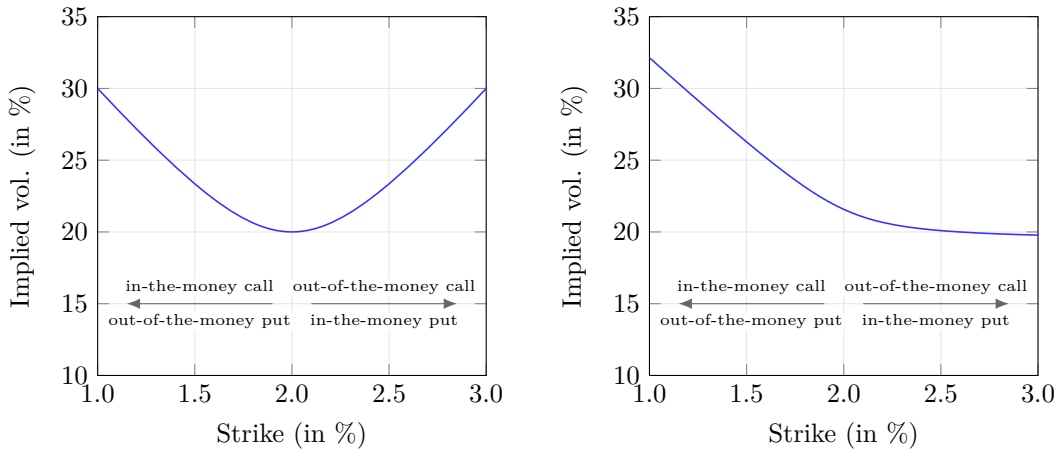
2.4.3 SABR Model

European options are often priced using Bachelier’s or Black’s model. In these models, there is a one-to-one relation between the price of an option and the volatility parameter. Consequently, option prices are often quoted by stating the implied volatility σ_N or σ_B , the unique value of the volatility which yields the option’s price when used in Bachelier’s or Black’s model, respectively. However, we often observe that the distribution of forward rates have heavier tails than implied by these models. This has the effect that there is no single implied volatility parameter anymore but rather a different implied volatility for every strike. In practice, the resulting curve resembles one of the two shapes shown below and is known as the volatility smile. Figure 2.1a shows that price of in-the-money or out-of-the-money option is relatively higher than the price of the corresponding at-the-money option, indicating heavier tails than predicted by Bachelier’s or Black’s model. Alternatively, when the volatility smile has a shape as in Figure 2.1b, it indicates that market participants want to protect themselves more against large downward movements, resulting in the higher volatilities for in-the-money call and out-of-the-money put options.

Managing the risks that arise from movements in the volatility smile is critical to fixed income trading desks, since these desks usually have large exposures across a wide range of strikes. To correctly capture the dynamics of the volatility smile, Hagan et al. [27] developed the SABR model, a stochastic volatility model in which the forward rate and volatility are correlated. So, the coefficient $c(t, \dots)$ from equation (2.20) is no longer deterministic. The dynamics of the SABR model are given by

$$\begin{aligned} dF(t) &= \alpha(t)(F(t))^\beta dW_1(t), & F(0) &= F_0, \\ d\alpha(t) &= \nu\alpha(t)dW_2(t), & \alpha(0) &= \alpha, \\ d\langle W_1, W_2 \rangle(t) &= \rho dt, \end{aligned} \quad (2.37)$$

where $\beta \in [0, 1]$, the initial volatility $\alpha > 0$, the volatility of volatility $\nu > 0$ and correlation $\rho \in (-1, 1)$. The β parameter is typically chosen by traders based on their beliefs on the evolution of the forward rate. The other three parameters are then chosen such that we match the market prices ‘as well as possible’ across all strikes.



- (a) Symmetric volatility smile. The implied volatility increases as the strike moves away from the forward rate.
- (b) Skewed volatility smile. The implied volatility decreases as the strike increases.

Figure 2.1: Typical shapes that arise when the implied volatility is plotted against the strike for options with the same expiry.

In general, there is no known closed form solution for the European option prices under the SABR model. However, one of the reasons that the SABR model is so popular is that Hagan et al. [27] derived approximating solutions for the normal and Black implied volatilities. These can then be used as input in Bachelier’s and Black’s formula. The approximating solution of Hagan et al. [27] was later improved by other researchers. In this thesis we use the version of Berestycki and Oblój [28, 35].

Theorem 2.25 (SABR formula). *Let $F(t)$ follow the dynamics from equation (2.37). Then the Black implied volatility σ_B is approximated by*

$$\sigma_B(F_0, K, T; \alpha, \rho, \nu, \beta) = I_0^B(1 + I_1^B T), \quad (2.38)$$

where

$$I_0^B = \frac{\nu \log(F_0/K)}{\log\left(\frac{\sqrt{1-2\rho z+z^2+z-\rho}}{1-\rho}\right)},$$

$$I_1^B = \frac{(1-\beta)^2}{24} \frac{\alpha^2}{(F_0 K)^{(1-\beta)}} + \frac{1}{4} \frac{\beta \alpha \rho \nu}{(F_0 K)^{(1-\beta)/2}} + \frac{2-3\rho^2}{24} \nu^2,$$

$$z = \begin{cases} \frac{\nu F_0^{1-\beta} - K^{1-\beta}}{\alpha(1-\beta)} & \text{if } \beta < 1, \\ \frac{\nu}{\alpha} \log(F_0/K) & \text{if } \beta = 1. \end{cases}$$

Proof. This was derived by Obloj [35], based on the theory from Berestycki [28]. \square

We can derive a similar approximating solution for the normal implied volatility σ_N of Bachelier's model, as shown by the following Theorem.

Theorem 2.26 (SABR formula). *Let $F(t)$ follow the dynamics from equation (2.37). Then the normal implied volatility σ_N is approximated by*

$$\sigma_N(F_0, K, T; \alpha, \rho, \nu, \beta) = I_0^N(1 + I_1^N T), \quad (2.39)$$

where

$$I_0^N = \frac{\nu(F_0 - K)}{\log\left(\frac{\sqrt{1-2\rho z+z^2+z-\rho}}{1-\rho}\right)},$$

$$I_1^N = \frac{\beta(\beta-2)}{24} \frac{\alpha^2}{(F_0 K)^{(1-\beta)}} + \frac{1}{4} \frac{\beta \alpha \rho \nu}{(F_0 K)^{(1-\beta)/2}} + \frac{2-3\rho^2}{24} \nu^2,$$

where z is as given in Theorem 2.25.

Proof. Note that by setting $\beta = 0$ and $\nu = 0$ the dynamics of the SABR model from equation (2.37), become equal to the dynamics of Bachelier's model from equation (2.32). So, by using Theorem 2.25 with $\beta = 0$ and $\nu = 0$, we have an approximation of Black's implied volatility for Bachelier's model

$$\lim_{\substack{\nu \rightarrow 0 \\ \beta \rightarrow 0}} \sigma_B(F_0, K, T; \sigma_N, \rho, \nu, \beta) = \frac{\log(F_0/K)}{F_0 - K} \sigma_N \left(1 + \frac{1}{24} \frac{\sigma_N^2}{F_0 K} T \right). \quad (2.40)$$

We can find the normal implied volatility σ_N for the SABR model by setting $\sigma_N = I_0^N(1 + I_1^N T)$ in equation (2.40). Through $\mathcal{O}(T^2)$ this yields

$$I_0^B(1 + I_1^B T) = \frac{\log(F_0/K)}{F_0 - K} I_0^N \left(1 + \left(I_1^N + \frac{1}{24} \frac{(I_0^N)^2}{F_0 K} \right) T \right) + \mathcal{O}(T^2). \quad (2.41)$$

Solving for I_0^N and I_1^N yields

$$\begin{aligned} I_0^N &= \frac{F_0 - K}{\log(F_0/K)} I_0^B, \\ I_1^N &= I_1^B - \frac{1}{24} \frac{(I_0^N)^2}{F_0 K} = I_1^B - \frac{1}{24} \frac{\alpha^2}{(F_0 K)^{1-\beta}}, \end{aligned} \quad (2.42)$$

where we used a similar approximation as Hagan et al. [27] did in their derivation of I_1^N . They use that for small ν , we have

$$I_0^N \approx \alpha(F_0 K)^{\beta/2}.$$

Plugging I_0^B and I_1^B from Theorem 2.25 into equation (2.42) proves the result. \square

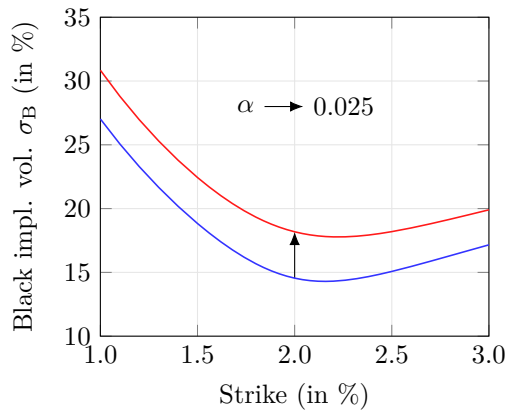
In the SABR model, the initial volatility α mainly affects the level of the volatility smile as can be seen in Figures 2.2a and 2.2b. A higher value of α yields a higher level of the volatility smile. The correlation ρ primarily affects the slope, where a lower value of ρ gives a steeper downward sloping smile, as can be seen in Figures 2.2c and 2.2d. The volatility of volatility ν mainly affects the curvature of the volatility smile as can be seen in Figures 2.2e and 2.2f.

Typically, we observe the implied volatilities $\widehat{\sigma}_B(F_0, K_i)$ or $\widehat{\sigma}_N(F_0, K_i)$ for a finite set K_i , $i = 1, \dots, n$, and fixed maturity T in the market. These are effectively the prices market participants are willing to buy or sell that specific option. In practice, we want to find SABR parameters that match these quotes. This process is called calibration and we do this by minimizing the sum of squared error's between market quoted implied volatilities and implied volatilities computed by the SABR model. So the SABR model parameters that match the market can be found by solving the optimization problem

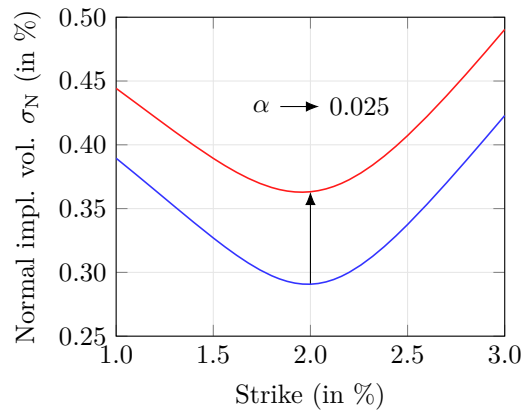
$$\arg \min_{\alpha, \rho, \nu} \sum_{i=1}^n (\widehat{\sigma}_B(F_0, K_i) - \sigma_B(F_0, K, T; \alpha, \rho, \nu, \beta))^2, \quad (2.43)$$

or

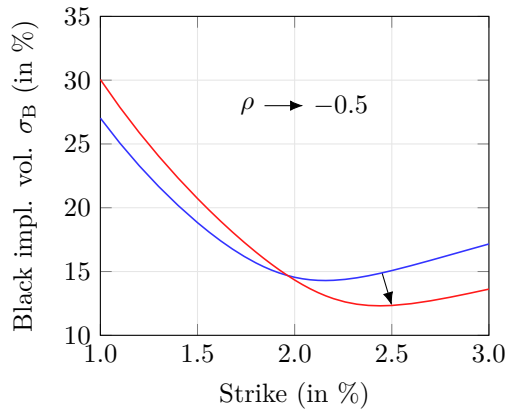
$$\arg \min_{\alpha, \rho, \nu} \sum_{i=1}^n (\widehat{\sigma}_N(F_0, K_i) - \sigma_N(F_0, K, T; \alpha, \rho, \nu, \beta))^2. \quad (2.44)$$



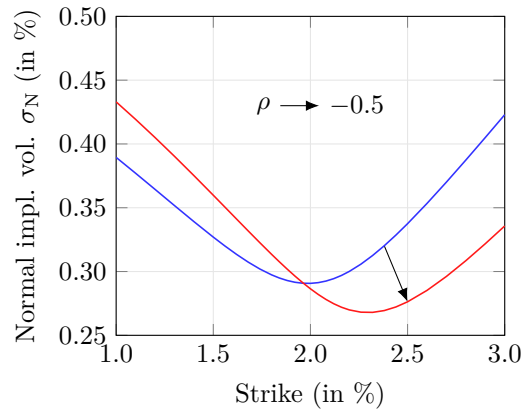
(a) Effect of the α parameter on the Black implied volatility σ_B .



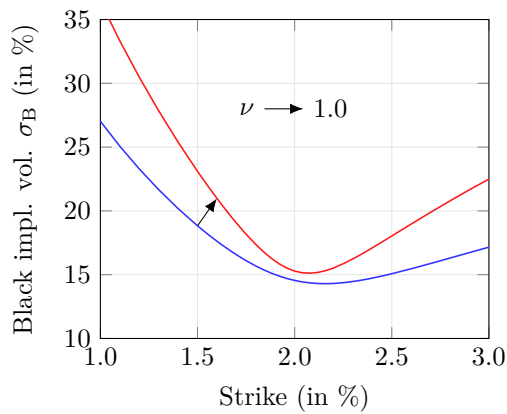
(b) Effect of the α parameter on the normal implied volatility σ_N .



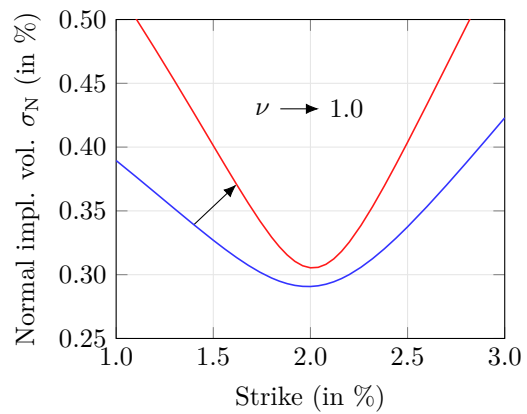
(c) Effect of the ρ parameter on the Black implied volatility σ_B .



(d) Effect of the ρ parameter on the normal implied volatility σ_N .



(e) Effect of the ν parameter on the Black implied volatility σ_B .



(f) Effect of the ν parameter on the normal implied volatility σ_N .

Figure 2.2: Effect of the SABR parameters on the implied volatility smile. Here the parameters are: $F_0 = 2\%$, $T = 1$ year, $\beta = 0.5$, $\alpha = 0.02$, $\rho = -0.1$, and $\nu = 0.6$.

Note that β is typically not included in the optimization. It turns out that we can find the same quality fit for any value of β . Therefore, β is typically chosen by traders based on their beliefs about the market or for aesthetic reasons.

To solve the optimization problem in equations (2.43) or (2.44) various methods exist. In this thesis, we will use the Levenberg-Marquardt algorithm [2, 3], since this algorithm is available in the standard distribution of Matlab.

2.4.3.1 Shifted SABR Model

When assuming the SABR model dynamics from equation (2.37), the forward rate cannot become negative. This poses the same problem as with Black's model. To solve this, we also add a small quantity to both the forward and the strike. This leads to the dynamics

$$\begin{aligned} dF(t) &= \alpha(t)(F(t) + s)^\beta dW_1(t), & F(0) &= F_0, & (2.45) \\ d\alpha(t) &= \nu\alpha(t)dW_2(t), & \alpha(0) &= \alpha, \\ d\langle W_1, W_2 \rangle(t) &= \rho dt, \end{aligned}$$

Modeling a forward rate with the shifted SABR model, allows the forward rate to be in the interval $(-s, \infty)$. So by choosing s positive, we can effectively allow for negative forward rates.

By a method similar to the one we used in the shifted Black model, we derive a similar approximation for the normal implied volatility σ_N . We also show how the shifted Black implied volatility σ_B^{sb} can be obtained, using a similar method as in [27], but instead applied to the shifted SABR model. As far as we know, the results from Theorem 2.27 and Theorem 2.28 cannot be found in the existing literature.

Theorem 2.27 (Shifted SABR formula). *Let $F(t)$ follow the shifted SABR model dynamics from equation (2.45). Then the normal implied volatility σ_N is approximated by*

$$\sigma_N(F_0, K, T; \alpha, \rho, \nu, \beta, s) = I_0^N(1 + I_1^N T), \quad (2.46)$$

where

$$\begin{aligned} I_0^N &= \frac{\nu(F_0 - K)}{\log\left(\frac{\sqrt{1-2\rho z+z^2+z-\rho}}{1-\rho}\right)}, \\ I_1^N &= \frac{\beta(\beta-2)}{24} \frac{\alpha^2}{((F_0+s)(K+s))^{(1-\beta)}} + \frac{1}{4} \frac{\beta\alpha\rho\nu}{((F_0+s)(K+s))^{(1-\beta)/2}} + \frac{2-3\rho^2}{24} \nu^2, \end{aligned}$$

$$z = \begin{cases} \frac{\nu}{\alpha} \frac{(F_0 + s)^{1-\beta} - (K + s)^{1-\beta}}{1 - \beta} & \text{if } \beta < 1, \\ \frac{\nu}{\alpha} \log((F_0 + s)/(K + s)) & \text{if } \beta = 1. \end{cases}$$

Proof. First note that Bachelier's formula, equations (2.33) and (2.35), are independent of shift. That is, for every $s \in \mathbb{R}$ we have

$$\begin{aligned} C_N(F_0, K, T, \sigma_N) &= C_N(F_0 + s, K + s, T, \sigma_N), \\ P_N(F_0, K, T, \sigma_N) &= P_N(F_0 + s, K + s, T, \sigma_N). \end{aligned}$$

So, if the normal implied volatilities σ_N are equal, then the option prices are equal, independent of the shift s . Now, if $F(t)$ follows the shifted SABR model dynamics from equation (2.45), then $F(t) + s$ follows the dynamics of the SABR model from equation (2.37). Therefore, we can apply the SABR formula, Theorem 2.26, to $F_0 + s$ and $K + s$. This proves the result. \square

Apart from an approximation for the normal implied volatility σ_N , we derive a new approximation formula for the shifted Black implied volatility σ_{BB}^s . This new formula allows us to compute the σ_{BB}^s when the SABR model was originally calibrated with another shift $s \neq s_{\text{B}}$. The ability to use different shifts will be very important in later parts of this thesis.

Theorem 2.28 (Shifted SABR formula). *Let $F(t)$ follow the shifted SABR model dynamics with shift s from equation (2.45). Then the implied volatility of the shifted Black model $\sigma_{\text{B}}^{s_{\text{B}}}$ with shift s_{B} is approximated by*

$$\sigma_{\text{B}}^{s_{\text{B}}}(F_0, K, T; \alpha, \rho, \nu, \beta, s) = I_0^{\text{B}}(1 + I_1^{\text{B}}T), \quad (2.47)$$

where

$$\begin{aligned} I_0^{\text{B}} &= \frac{\nu \log((F_0 + s_{\text{B}})/(K + s_{\text{B}}))}{\log\left(\frac{\sqrt{1-2\rho z+z^2+z-\rho}}{1-\rho}\right)}, \\ I_1^{\text{B}} &= \frac{1}{24} \frac{\alpha^2}{((F_0 + s_{\text{B}})(K + s_{\text{B}}))^{(1-\beta)}} + \frac{\beta(\beta-2)}{24} \frac{\alpha^2}{((F_0 + s)(K + s))^{(1-\beta)}} \\ &\quad + \frac{1}{4} \frac{\beta\alpha\rho\nu}{((F_0 + s)(K + s))^{(1-\beta)/2}} + \frac{2-3\rho^2}{24} \nu^2, \\ z &= \begin{cases} \frac{\nu}{\alpha} \frac{(F_0 + s)^{1-\beta} - (K + s)^{1-\beta}}{1 - \beta} & \text{if } \beta < 1, \\ \frac{\nu}{\alpha} \log((F_0 + s)/(K + s)) & \text{if } \beta = 1. \end{cases} \end{aligned}$$

Proof. Note that by setting $\beta = 1$ and $\nu = 0$, the dynamics of the shifted SABR model with shift s_B from equation (2.45), become equal to the dynamics of the shifted Black model from equation (2.29). So, by using Theorem 2.27 with $\beta = 1$ and $\nu = 0$, we have an approximation of the normal implied volatility for the shifted Black model.

$$\lim_{\substack{\nu \rightarrow 0 \\ \beta \rightarrow 1}} \sigma_N(F_0, K, T; \sigma_B^{s_B}, \rho, \nu, \beta, s) = \frac{F_0 - K}{\log\left(\frac{F_0 + s_B}{K + s_B}\right)} \sigma_B^{s_B} \left(1 - \frac{1}{24} (\sigma_B^{s_B})^2 T\right). \quad (2.48)$$

We can find the shifted Black implied volatility $\sigma_B^{s_B}$ for the SABR model by setting $\sigma_B^{s_B} = I_0^B(1 + I_1^B T)$ in equation (2.48). Through $\mathcal{O}(T^2)$ this yields

$$I_0^N (1 + I_1^N T) = \frac{F_0 - K}{\log\left(\frac{F_0 + s_B}{K + s_B}\right)} I_0^B \left(1 + \left(I_1^B - \frac{1}{24} (I_0^B)^2\right) T\right) + \mathcal{O}(T^2). \quad (2.49)$$

Solving for I_0^B and I_1^B yields

$$\begin{aligned} I_0^B &= \frac{\log((F_0 + s_B)/(K + s_B))}{F_0 - K} I_0^N, \\ I_1^B &= I_1^N + \frac{1}{24} (I_0^B)^2 = I_1^N + \frac{1}{24} \frac{\alpha^2}{((F_0 + s_B)(K + s_B))^{1-\beta}}, \end{aligned} \quad (2.50)$$

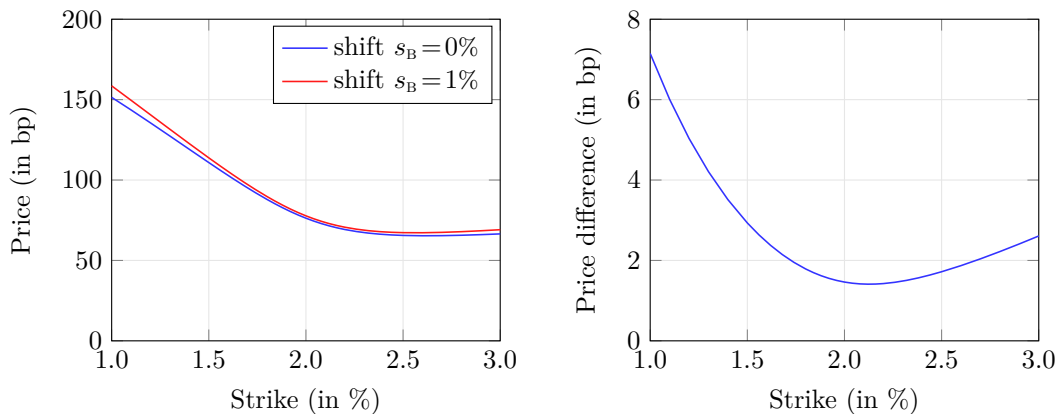
where we used a similar approximation as Hagan et al. [27] did in their derivation of I_1^N . They use that for small ν we have

$$I_0^B \approx \frac{\alpha}{((F_0 + s_B)(K + s_B))^{(1-\beta)/2}}.$$

Plugging I_0^N and I_1^N from equation (2.46) with shift s into equation (2.50), proves the result. \square

Note that Theorem 2.28 an approximation that is most accurate for small maturities. Therefore, we expect small differences in the option price depending on the shifted Black implied volatility $\sigma_B^{s_B}$ that is used to obtain that price, especially for larger maturities. So, when a different shift s_B is used we also expected to see a slightly different price.

To see this effect we compared option prices obtained with different values for the shift s_B , using a large maturity $T = 20$ years. As can be seen in Figure 2.3, the prices obtained depend slightly on the shift parameter that is used. Since the price difference stays within a few basis points across a wide range of strikes and will be even less for smaller maturities we conclude that these errors are small enough for the applications in this thesis.



(a) Prices obtained with different shift s_B . (b) Difference between the prices in (a).

Figure 2.3: Prices in basis points when using different values for the shift s_B in Theorem 2.28 with constant SABR parameters. Here the parameters are: $F_0 = 2\%$, $s = 0\%$, $T = 20$ years, $\beta = 0.5$, $\alpha = 0.02$, $\rho = -0.1$, and $\nu = 0.6$.

2.5 Bootstrapping Market Data

So far, we have assumed that all forward rates $L_i(0)$ and forward swap rates $S_{n,m}(0)$ are known. In practice, only spot rates are quoted in the market. In this section, we discuss a method to compute the forward rates $L_i(0)$ and forward swap rates $S_{n,m}(0)$ that are consistent with the current spot rates $L_0(0)$ and $S_{0,m}(0)$ observed in the market. The results can be presented in various forms

- (a) As a function $T_i \mapsto P(0, T_i)$; this is called the discount curve or zero-coupon curve.
- (b) As a function $T_i \mapsto L_i(0)$, assuming that all tenors $T_{i+1} - T_i$ are equal; this is called the forward curve.
- (c) As a function $T_n \mapsto S_{n,m}(0)$, assuming that the swap tenor $T_m - T_n$ stays equal; this is called the forward swap curve.

The simplest method of doing this involves a method known as bootstrapping. This method works by incrementally computing zero-coupon bonds in order of increasing maturity. Once we have all zero-coupon bond prices, we can use Definition 2.5 to compute the forward rates

$$L_i(0) = \frac{1}{\tau_i} \left(\frac{P(0, T_i)}{P(0, T_{i+1})} - 1 \right), \quad (2.51)$$

and Definition 2.6 to compute the forward swap rates

$$S_{n,m}(0) = \frac{P(0, T_n) - P(0, T_m)}{A_{n,m}(0)}. \quad (2.52)$$

By definition of the zero-coupon, bond we have that $P(0,0) = 1$. Now we can compute the first zero-coupon bond from the spot rate as

$$L_0(0) = \frac{1}{\tau_0} \left(\frac{1}{P(0, T_1)} - 1 \right), \quad \Leftrightarrow \quad P(0, T_1) = \frac{1}{1 + \tau_0 L_0(0)}.$$

The next zero-coupon bonds can be computed from the spot swap rates. These are typically quoted for maturities T_m up to 30 years or more. By equation 2.52, the spot swap rate is given by

$$S_{0,m}(0) = \frac{1 - P(0, T_m)}{\sum_{i=0}^{m-1} \tau_i P(0, T_{i+1})}.$$

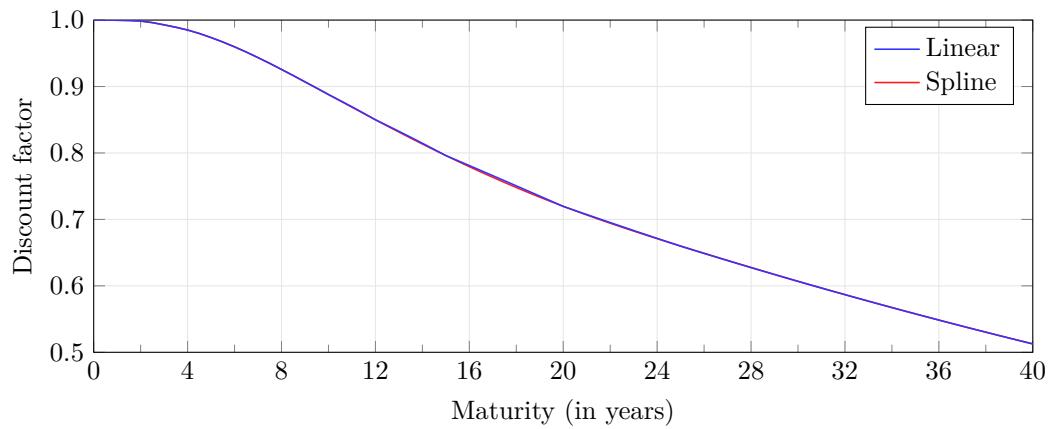
By rewriting this, we get

$$\begin{aligned} 1 - P(0, T_m) &= S_{0,m}(0) \left(\sum_{i=0}^{m-2} \tau_i P(0, T_{i+1}) + \tau_{m-1} P(0, T_m) \right), \quad \Leftrightarrow \\ P(0, T_m) &= \frac{1 - S_{0,m}(0) \sum_{i=0}^{m-2} \tau_i P(0, T_{i+1})}{1 + \tau_{m-1} S_{0,m}(0)}. \end{aligned}$$

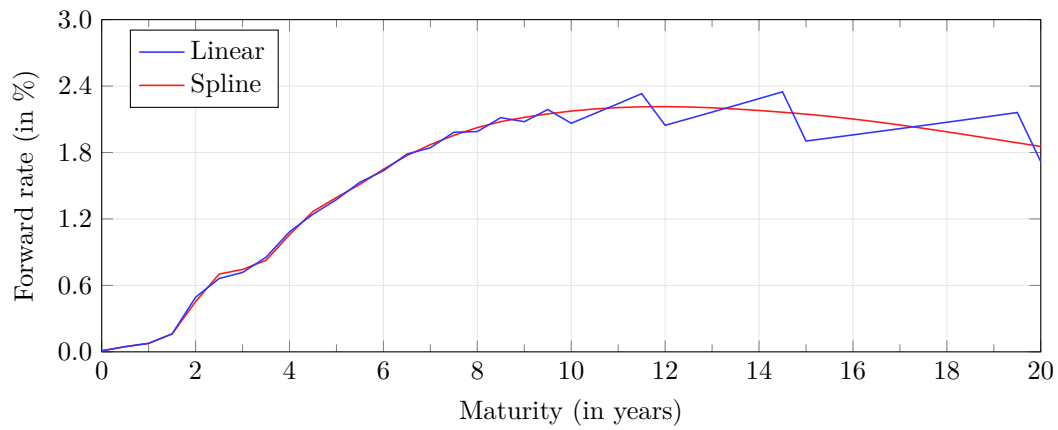
This allows us to compute the value of the n th zero-coupon bond based on the n th swap rate and the previous $n - 1$ zero-coupon bonds. The value of zero-coupon bonds $P(0, t)$, with $T_{n-1} < t < T_n$, can be found by interpolation.

In practice, not all swap rates are quoted and the swap rates for some maturities T_m can be missing. To determine the missing swap rates, an interpolation method needs to be used. In Figure 2.4, linear interpolation is compared with C^2 -spline interpolation [37]. As can be seen in Figure 2.4b, linear interpolation can give a jagged curve that Filipović referred to as a “sawtooth” shape [36], This indicates that linear interpolation of the swap rates might be inappropriate to compute the forward rates in some cases. On the other hand, using spline interpolation gives a smoother curve, but the resulting forward rates become very sensitive to the data. In this thesis, we will use the linear interpolation because it is more robust than the spline based method. Note that both interpolation methods exactly reconstruct market prices which is often a desirable property.

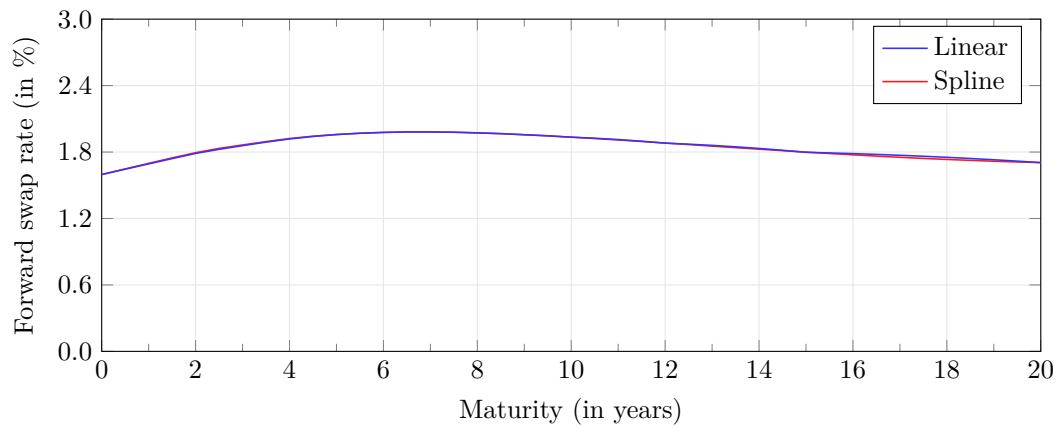
There are still other possibilities. When the data is questionable, we can allow for small pricing errors in favor of a more robust estimation method. Some options include fitting a parametric curve to force the forward rates into an idealized form, as suggested by Nelson and Siegel [11], and Svensson [13] or non-parametric methods such as smoothing splines, described in [37]. These methods, however, are beyond the scope of this thesis.



(a) Bootstrapped zero-coupon curve.



(b) Bootstrapped 6m forward curve.



(c) Bootstrapped forward swap curve with swap tenor of 20y.

Figure 2.4: Bootstrapped discount curve (a), forward curve (b), and forward swap curve (c) based on Euribor rates and swaps with Euribor as reference rate from 18-06-2015.

Chapter 3

Risk Measurement

In this chapter, we will show how market risk is measured. This is the risk of loss due to unforeseen changes in market prices and market rates. Quantifying and accurately measuring this type of risk is very important, since the amount of capital that needs to be set aside is primarily based on the measured market risk.

We start this chapter by introducing risk measures and the properties they should satisfy. After that we show how these measures can be computed using the historical simulation method. We end this chapter with different backtesting methods that can be used to validate the computed risk measures.

3.1 Risk Measures

When measuring market risk, we look at the monetary risk of a specific portfolio. That is the risk of a decrease in market value of that portfolio. To this end, we look at the portfolio's profits and losses. The profit and loss is the difference between the portfolio's value at two different points in time. Typically, the portfolio's current value is compared with its value h trading days later, where h is called the risk horizon.

In order to define the profit and loss, let $V(t)$ be the value of a given portfolio at time t . The difference between $V(t)$ and $V(t+h)$ is the time t profit and loss. In practice, t is today, so that $t+h$ is some date in the future and therefore not yet known. In this case, $V(t+h)$ has to be estimated and the profit and loss will be a random variable.

Definition 3.1 (Profit and loss distribution). For a given portfolio, the profit and loss distribution at time t , with a risk horizon of h trading days, is given by

$$X = X(t, h) = V(t+h) - V(t). \quad (3.1)$$

As mentioned above, we look at the profit and loss of today, so if today is T_0 , then we consider $X(T_0, h)$. The risk horizon is commonly set to either 1 trading day or 10 trading days, which equals 2 weeks.

Remark 3.2. If we want to be precise in our definition of the profit and loss distribution, we should also consider the time value of money. To this end, we should have discounted the portfolio's time $t + h$ value as explained in Section 2.1. To be completely correct, we should use $X(t, h) = P(t, t + h)V(t + h) - V(t)$ instead, where $P(t, t + h)$ is the time t zero-coupon bond with maturity $t + h$. However, since h is typically small, the effect of considering the time value of money is negligible and not worth the extra complexity. Therefore, we will keep using Definition 3.1 in the rest of this thesis. \triangle

3.1.1 Monetary and Coherent Risk Measures

Before we introduce concrete examples of risk measures, we first define the properties that a risk measure should satisfy. The aim is to quantify the amount of monetary risk for a given portfolio as an amount of extra capital that should be set aside in order to make the risk of loss acceptable from the point of view of a supervisory agency. So, in order to define a monetary risk measure, we let \mathcal{X} be the set of profit and loss distributions of all portfolios at time T_0 .

Definition 3.3 (Monetary risk measure). A function $\rho : \mathcal{X} \rightarrow \mathbb{R}$ is a monetary risk measure if for all $X, Y \in \mathcal{X}$ we have

$$\begin{aligned} \rho(X) &\geq \rho(Y) && \text{for } X \leq Y \text{ a.s.,} && \text{(Monotonicity)} \\ \rho(X + m) &= \rho(X) - m && \text{for } m \in \mathbb{R}. && \text{(Translation invariance)} \end{aligned}$$

A portfolio with profit and loss distribution X is called acceptable when $\rho(X) \leq 0$.

The financial interpretation of the monotonicity property is that a portfolio that always has a higher profit should be considered less risky. Translation invariance is motivated by the interpretation of ρ as a capital requirement. This means that the portfolio should become acceptable by adding a risk-free amount $\rho(X)$ to the portfolio. By translation invariance this is guaranteed, since $\rho(X + \rho(X)) = \rho(X) - \rho(X) = 0$.

Although a monetary risk measure clearly defines a risk measure that can be used as a capital requirement, it does not capture all aspects we would expect from a risk measure. For example, diversification of a portfolio should not increase risk. To this end, Artzner et al. have introduced the concept of coherent risk measures [20], which was later generalized by Föllmer and Schied [26, 34].

Definition 3.4 (Coherent risk measure). A monetary risk measure ρ is a coherent risk measure, if for all $X, Y \in \mathcal{X}$ we have

$$\begin{aligned} \rho(\lambda X + (1 - \lambda)Y) &\leq \lambda \rho(X) + (1 - \lambda)\rho(Y), & \text{for } 0 \leq \lambda \leq 1, & \quad (\text{Convexity}) \\ \rho(\alpha X) &= \alpha \rho(X), & \text{for } 0 \leq \alpha. & \quad (\text{Positive homogeneity}) \end{aligned}$$

The convexity property directly captures the idea that diversification should decrease risk. Indeed, the risk of the diversified position $\lambda X + (1 - \lambda)Y$ should be less than or equal to the weighted average of the individual positions λX and $(1 - \lambda)Y$. The financial meaning of positive homogeneity is that the size of the portfolio is directly proportional to the size of the risk. Especially, the risk of holding no assets should be zero, i.e. $\rho(0) = 0$. Also note that positive homogeneity together with convexity implies the property

$$\rho(X + Y) \leq \rho(X) + \rho(Y). \quad (\text{Sub-additivity})$$

This allows for the decentralization of risk measurement. Often a large financial institution has to manage risks which are divided over many different portfolios. By setting risk limits on each portfolio, the sub-additive property ensures that the total risk does not exceed the sum of these limits.

3.1.2 Value at Risk

The first concrete example of a risk measure we give is the value at risk, which is currently the most widely used risk measure. The main reason is that the Basel Committee on Banking Supervision made value at risk the preferred risk measure in their Basel II accord [29]. Because of this, the amount of capital that financial institutions need to set aside is directly proportional to the value at risk. So, it has become increasingly important to compute the value at risk as accurately as possible.

The value at risk is the amount of monetary loss of a given portfolio that is exceeded only a small amount of the time within a fixed time horizon. In this case, ℓ is called the significance level and is set by the Basel Committee to be 1% [29].

To formally define the value at risk, we first introduce quantiles and the quantile function. A ℓ -quantile of a random variable X is any value x such that $\mathbb{P}(X \leq x) = \ell$. The quantile function is then the infimum among all quantiles of a given level. So the quantile function of X is given by

$$Q_X(\ell) = \inf \{x \in \mathbb{R} \mid \mathbb{P}(X \leq x) \geq \ell\}. \quad (3.2)$$

The value at risk is then the negative value of the smallest quantile of a given profit and loss distribution at the given significance level ℓ .

Definition 3.5 (Value at Risk). For a given significance level $\ell \in (0, 1)$, or confidence level $1 - \ell$, and a risk horizon h , the value at risk of a portfolio with today's profit and loss distribution $X = X(T_0, h)$ is given by

$$\text{VaR}_X(\ell) = -Q_X(\ell) = -\inf \{x \in \mathbb{R} \mid \mathbb{P}(X \leq x) \geq \ell\}, \quad (3.3)$$

where \mathbb{P} is the real-world probability measure.

It can be easily checked that the value at risk is a monetary risk measure that also satisfies the positive homogeneity property. Also, when the profit and loss distribution is normal, or more general when it has an elliptical distribution, it can be shown that the value at risk is sub-additive [32]. However, in general the value at risk is not sub-additive and hence it is not a coherent risk measure, as shown by the following example.

Example 3.6. Consider two instruments that each have a probability of 4% to incur a loss of €1000 independently of each other, otherwise they make a profit of €50. When we compute the 5% value at risk for each product separately, we see that it is minus €50. So, when considered separately both products will be deemed acceptable. However, when we consider both products together, the probability that at least one will incur a loss is $1 - (1 - 0.04)^2 \approx 7.8\%$. So, in this case the 5% value at risk will be at least €950. Therefore, the value at risk of both products combined is larger than zero and hence not acceptable. Hence, the value at risk is not a sub-additive risk measure. \triangle

Note that the example above relies on large jumps in the profit and loss distribution, which might not be realistic for a large portfolio. However, there are various other examples showing that the value at risk is not sub-additive even when the profit and loss distribution is continuous [32, 31, 33].

What this example shows, is that the value at risk ignores the severity of the losses below the significance level and therefore may fail to stimulate diversification. The value at risk also does not account for the severity of the losses. This is troubling from a regulatory point of view as the losses beyond the significance level are typically those where the regulator has to step in.

3.1.3 Expected Shortfall

Due to the shortcomings of value at risk the Basel Committee on Banking Supervision is planning to stop using value at risk for capital requirements. Under the Basel III regulations the capital requirements will be based on the expected shortfall measure with a significance level $\ell = 2.5\%$ [48, 39].

The expected shortfall is defined as the average of all value at risk up to a certain significance level. This leads to the following definition.

Definition 3.7 (Expected shortfall). For a given significance level $\ell \in (0, 1)$, or confidence level $1 - \ell$, and a risk horizon h , the expected shortfall of a portfolio with today's profit and loss distribution $X = X(T_0, h)$ is given by

$$\text{ES}_X(\ell) = \frac{1}{\ell} \int_0^\ell \text{VaR}_X(u) du. \quad (3.4)$$

Note that the expected shortfall is continuous in its significance level, i.e. the function $\ell \mapsto \text{ES}_X(\ell)$ is continuous. Because there are no jumps in the expected shortfall, it is less sensitive to the choice of significance level than the value at risk.

When the profit and loss distribution X is continuous, we have a more intuitive representation for the expected shortfall as shown in Lemma 3.8. This shows that the expected shortfall can be written as the average loss, given that the loss exceeds the value at risk.

Lemma 3.8. *Let X be a continuous profit and loss distribution of some portfolio, then the expected shortfall can also be written as*

$$\text{ES}_X(\ell) = -\mathbb{E}[X \mid X \leq -\text{VaR}_X(\ell)], \quad (3.5)$$

where \mathbb{E} is the expectation under the real-world probability measure.

Proof. Since X has a continuous distribution we have $\text{VaR}_X(\ell) = -F^{-1}(\ell)$, where F^{-1} denotes the inverse cumulative distribution function of X . Then by substituting $u = F(x)$ we find

$$\begin{aligned} \int_0^\ell \text{VaR}_X(u) du &= - \int_0^\ell F^{-1}(u) du \\ &= - \int_{-\infty}^{F^{-1}(\ell)} x dF(x) \\ &= -\mathbb{E}[X \mid X \leq F^{-1}(\ell)] \mathbb{P}(X \leq F^{-1}(\ell)) \\ &= -\mathbb{E}[X \mid X \leq -\text{VaR}_X(\ell)] \mathbb{P}(X \leq -\text{VaR}_X(\ell)). \end{aligned}$$

Also, since X has a continuous distribution, we have that $\mathbb{P}(X \leq -\text{VaR}_X(\ell)) = \ell$ and the result follows. \square

The representation from Lemma 3.8 shows that the expected shortfall is based on the tail of the profit and loss distribution X , in contrast to the value at risk, which is based on a single point of the profit and loss distribution. So, the expected shortfall

also takes the severity of the losses beyond the value at risk into account. This property is especially important for regulators who have to step in when the losses become too severe for an institution to handle themselves.

Similar to value at risk, it is also easy to see that expected shortfall is a monetary risk measure that satisfies the positive homogeneity property. Moreover, Acerbi and Tasche have shown that the expected shortfall does also satisfy the sub-additivity property [24, 23]. Hence, the expected shortfall is a coherent risk measure, as it possesses all the properties we expect from a risk measure.

3.2 Estimating Profit and Loss

In order to compute the value at risk or expected shortfall, we need to estimate today's profit and loss distribution $X = X(T_0, h)$, where today is denoted by T_0 . In this thesis, we will use the historical simulation method, first introduced by Hendricks [14] and currently the most used method to estimate profit and loss distributions. Perignon and Smith showed that approximately 3 out of every 4 commercial banks use historical simulation [38].

The main advantage of historical simulation is that it does not make any assumptions on the shape profit and loss distribution and that it is relatively easy to implement. However, since a historical simulation is based on historical data, we do make the implicit assumption that the historical market changes are representative for today. That is, we assume normal market conditions to allow the use of past observations to determine likely future scenarios.

3.2.1 Historical Simulation

A historical simulation consists of generating n possible future market scenarios, based on historical observations. In each of these scenarios, we determine the portfolio's value based on the market values in that scenario. Then, by subtracting the portfolio's current value, we find a set of possible profits and losses. These profits and losses are then combined to form an empirical distribution from which the value at risk or expected shortfall can be computed.

To formally define historical simulation, we first need to determine a set of market prices and market rates, which determine the value of our portfolio. All market prices and market rates that are relevant to the portfolio's value will be called risk factors. The value of all risk factors at time t will be stored in a d dimensional vector $R \in \mathbb{R}^d$.

We also need a calibration window, this is the historical period that will be used to generate the values of each risk factor. To this end let t_i , with $i = 1, \dots, n + m$, be

a set of daily historical observation times such that $t_i \leq T_0$ and $t_i - t_{i-m} = h$ for all i . With historical simulation we require $R(T_0)$ and $R(t_i)$, for $i = 1, \dots, n + m$, to be known.

We then generate n different future scenarios by applying historically observed shocks to the current risk factor values. Let $\hat{R}^i(T_0 + h)$ denote the risk factor values in the i th scenario. Then $\hat{R}^i(T_0 + h)$ can be computed by

$$\hat{R}^i(T_0 + h) = R(T_0) + \underbrace{R(t_{i+m}) - R(t_i)}_{\text{historical shock}}, \quad \text{for all } i = 1, \dots, n. \quad (3.6)$$

So, we assume that shocks which occurred in the past, will be similar to the shocks happening today. Example 3.9 shows how a scenario is generated by applying shocks to risk factors.

Example 3.9. Suppose that we only have one single risk factor, so $R(t)$ is a single number. Figure 3.1 gives an example of a hypothetical risk factor with $n = 10$ different daily observations. In this example, we want to estimate the profit and loss distribution with risk horizon $h = 1$ day, so $m = 1$. In this example, we have $R(T_0) = 2$ as the current value of the risk factor. As can be seen in Figure 3.1, the first historical values of this risk factor are $R(t_0) = 5$, $R(t_1) = 7$, $R(t_2) = 6$, and $R(t_3) = 3$. Therefore, the first three scenarios will be

$$\begin{aligned} R_1(T_0 + h) &= 2 + 7 - 5 = 4, \\ R_2(T_0 + h) &= 2 + 6 - 7 = 1, \\ R_3(T_0 + h) &= 2 + 3 - 6 = -1. \end{aligned} \quad \triangle$$

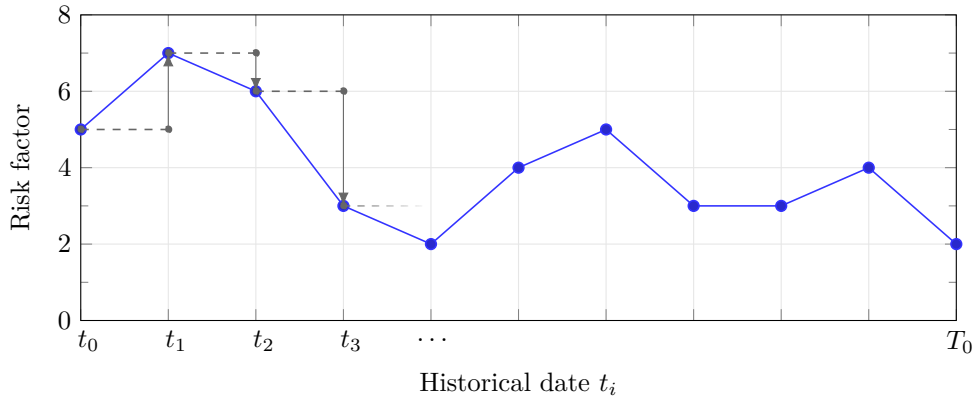


Figure 3.1: Example of how to calculate shocks from risk factor values. The shocks are represented by the gray arrows. In this example the risk horizon is 1 day and the first three shocks are: +2, -1 and -3.

As we will see later, some risk factors should always be positive even after applying historical shocks. This can be accomplished using so called relative shocks. To apply a relative shock, we use a log-transformation before applying the historical shock. Then the j th risk factor $\hat{R}_j^i(T_0 + h)$ can be computed by

$$\begin{aligned} \log(\hat{R}_j^i(T_0 + h)) &= \log(R_j(T_0)) + \log(R_j(t_{i+m})) - \log(R_j(t_i)), & (3.7) \\ &\Downarrow \\ \hat{R}_j^i(T_0 + h) &= R_j(T_0) \cdot \left(1 + \frac{R_j(t_{i+m}) - R_j(t_i)}{R_j(t_i)}\right), \quad \text{for all } i = 1, \dots, n. \end{aligned}$$

Once we have created all scenarios, we need to determine the portfolio's value in each of those scenarios. We will use $V_i(T_0 + h)$ to denote the value of the portfolio, given that the market will be equal to that of the i th scenario, i.e. we assume that the market is given by the values in $\hat{R}^i(T_0 + h)$. Then the profit and loss in each scenario is given by

$$X_i = V_i(T_0 + h) - V(T_0), \quad \text{for all } i = 1, \dots, n. \quad (3.8)$$

The X_i can be interpreted as samples from the actual (unknown) profit and loss distribution X . These samples can then be used to create an empirical distribution or to estimate the value at risk and expected shortfall directly.

Generating more samples will theoretically increase the accuracy of the estimation. However, in order to simulate more samples we need a larger calibration window and hence more historical data, which might not be available. Moreover, historical data from long ago might not be representative for today due to possible changes in the market or in regulation. Therefore, we need to be prudent in the choice of calibration window. In this thesis, we will use a calibration window of one year of daily observations, as prescribed by the Basel II accord [29].

3.2.2 Value at Risk Estimation

Given n samples (X_1, \dots, X_n) of the profit and loss distribution X , we want to estimate the value at risk from Definition 3.5. To this end, let $X_{(1)} \leq \dots \leq X_{(n)}$ be the order statistics of this sample, so $X_{(i)}$ is the i th smallest sample from the set (X_1, \dots, X_n) . Also let $\lfloor x \rfloor$ be the integer part of x , that is

$$\lfloor x \rfloor = \max \{n \in \mathbb{Z} \mid n \leq x\}.$$

A natural estimator for the value at risk is then the $\lfloor n\ell \rfloor$ th order statistic, where n is the number of samples and ℓ is the significance level. So, the value at risk, based

on n samples, can be estimated by

$$\text{VaR}(\ell) = -X_{(\lfloor n\ell \rfloor)}. \quad (3.9)$$

When the profit and loss distribution is not continuous, the estimator from equation (3.9) is not consistent [4]. Nevertheless, in practical applications the profit and loss distribution will only have small discontinuities, so the estimator from equation (3.9) is a good approximation to the real value at risk.

3.2.3 Expected Shortfall Estimation

In order to estimate the expected shortfall, we use the representation from Lemma 3.8. Therefore, the expected shortfall, based on n samples, can be estimated by

$$\text{ES}(\ell) = -\frac{1}{\lfloor n\ell \rfloor} \sum_{i=1}^{\lfloor n\ell \rfloor} X_{(i)}. \quad (3.10)$$

Although we need the profit and loss distribution to be continuous for Lemma 3.8 to hold, it was shown by Acerbi and Tasche that the estimator from equation (3.10) is a consistent even when the profit and loss distribution is not continuous [24].

3.3 Backtesting

Backtesting is the process of testing the correctness of an estimation procedure. In our case, this means that we compare the actual profits or losses with the estimated value at risk or expected shortfall. We can then test whether a certain estimation method is likely to be correct based on statistical analysis. In this section, we present several different backtesting methods. We start by describing how to backtest the value at risk, after which we continue by extending those approaches, so that they can also be used to backtest the expected shortfall.

3.3.1 Backtesting Value at Risk

Backtests for value at risk are defined by comparing the realized profit and loss against the estimated value at risk. This comparison is typically done using the value at risk failure indicator that equals 1 when the realized loss exceeds the value at risk estimate and 0 otherwise. So, the value at risk failure indicator is defined as follows.

Definition 3.10 (VaR Failure indicator). Let x_i , with $i = 1, \dots, N$, be the realized profit or loss at day i and let $\text{VaR}_i(\ell)$ be the forecasted value at risk for that day. Then, the value at risk failure indicator is given by

$$H_{\text{VaR}(\ell)}^{(i)} = \mathbb{1}_{\{-x_i \geq \text{VaR}_i(\ell)\}}, \quad (3.11)$$

where $\mathbb{1}$ is used to denote the indicator function.

As shown by Christoffersen, determining the accuracy of a value at risk method can now be reduced to the problem of checking if the failure indicators $H_{\text{VaR}(\ell)}^{(i)}$ satisfy the following two properties [19, 30].

- *Unconditional coverage property.* The probability of exceeding the value at risk should be equal to the significance level ℓ . Therefore, a value at risk model can be deemed accurate if $\mathbb{P}(H_{\text{VaR}(\ell)}^{(i)} = 1) = \ell$. If the probability of exceeding the value at risk is higher than ℓ , the value at risk model is underestimating the portfolio's actual risk. The alternative is that this probability is lower than ℓ , which indicates that the value at risk is too conservative, resulting in an unnecessarily high value at risk.
- *Independence property.* The unconditional coverage property places a restriction on the average number of value at risk violations. For a value at risk model to be correct, we also need the failure indicators to be spaced independently throughout time. Specifically, there should be no correlation between two failure indicators $H_{\text{VaR}(\ell)}^{(i)}$ and $H_{\text{VaR}(\ell)}^{(j)}$, when $i \neq j$. Suppose, for example, that value at risk violations always occur in pairs, then if the value at risk was exceeded today, we know that we will exceed it again tomorrow with certainty. Hence, in this case the value at risk does not accurately reflect the risk of the portfolio. In general, a clustering of value at risk violations indicates that the independence property is not satisfied because the value at risk model does not adjust to changing market conditions quickly enough, making successive value at risk violations more likely.

Although a good value at risk model should satisfy both the unconditional coverage property and the independence property, the unconditional coverage property is considered more important. This is confirmed by the Basel Committee on Banking Supervision by requiring only to test the unconditional coverage property [29]. Nevertheless, in this thesis we will perform backtests that check both of these properties.

3.3.1.1 Unconditional Coverage

An unconditional coverage test is used to check if the total amount of times the value at risk has been exceeded is reasonable. When the value at risk is exceeded too often, it might indicate that we are systematically underestimating risk. On the other

hand, when the number of value at risk violations is too low, we are overestimating the risk. To this end, statistical tests can provide valuable insight in the quality of the estimation method.

When the number of backtesting days N is large enough, we can use a simple Z -test to check the validity of the value at risk estimate [50, 49].

Theorem 3.11. *If the value at risk model is correct, the failure indicator $H_{\text{var}(\ell)}^{(i)}$ from Definition 3.10, is asymptotically normal with mean ℓ and variance $\ell(1 - \ell)$ and therefore admits a Z -test, with Z -score given by*

$$Z = \sqrt{N} \frac{\left(\frac{1}{N} \sum_{i=1}^N H_{\text{var}(\ell)}^{(i)} \right) - \ell}{\sqrt{\ell(1 - \ell)}}. \quad (3.12)$$

Proof. Under the assumption that the value at risk model is correct, all failure indicators $H_{\text{var}(\ell)}^{(i)}$ are Bernoulli random variables with probability ℓ . Hence, each failure indicator has mean ℓ and variance $\ell(1 - \ell)$. It then follows by the central limit theorem that

$$Z = \sqrt{N} \frac{\left(\frac{1}{N} \sum_{i=1}^N H_{\text{var}(\ell)}^{(i)} \right) - \ell}{\sqrt{\ell(1 - \ell)}} \xrightarrow[N \rightarrow \infty]{d} \mathcal{N}(0, 1).$$

That is, Z converges in distribution to a standard normal distribution. So, for a large enough sample size N , we can use a Z -test. \square

The Z -score from equation (3.12) can now be used to define one-sided or two-sided Z -test through the standard normal cumulative distribution Φ . In case we only worry about the underestimation of risk, a one-sided test can be defined by $p = \Phi(-Z)$. When we are also concerned about overestimation, we can use a two-sided test as $p = 2\Phi(-|Z|)$. When these p -values become too small, it is unlikely that the value at risk model is correct and we can reject the validity of that model.

3.3.1.2 Independence

The unconditional coverage test only checks if the total amount of value at risk violations is close to the expected value. However, we also want to check if the violations are independent throughout time. Exceeding the value at risk multiple consecutive days may be an indicator that our estimation procedure is inadequate. Hence, when we see too many value at risk violations clustered, this could be the basis of rejecting a certain model.

To check whether the value at risk exceedances are not clustered throughout time, we will describe a method based on the backtest by Du and Escanciano [50]. This can be

done by checking if there is no serial correlation in the value at risk failure indicator process $H_{\text{VaR}(\ell)}^{(i)}$. Using the Ljung-Box statistic, we can test for this kind a correlation up to a certain number of lags m [8]. That is, we test if there is any correlation between the failure indicator $H_{\text{VaR}(\ell)}^{(i)}$ at day i and $H_{\text{VaR}(\ell)}^{(i-k)}$, for $k = 1, \dots, m$.

Definition 3.12 (Ljung-Box statistic). Let $H_{\text{VaR}(\ell)}^{(i)}$ be the value at risk failure indicator, for $i = 1, \dots, N$, and let m be a number of lags. Then, the Ljung-Box test statistic is given by

$$Q = N(N + 2) \sum_{k=1}^m \frac{\rho_k^2}{N - k}, \quad (3.13)$$

where

$$\rho_k = \frac{\sum_{i=k+1}^N \left(H_{\text{VaR}(\ell)}^{(i)} - \ell \right) \left(H_{\text{VaR}(\ell)}^{(i-k)} - \ell \right)}{\sum_{i=1}^N \left(H_{\text{VaR}(\ell)}^{(i)} - \ell \right)^2}.$$

Under the hypothesis that all failure indicators are independent, i.e. that there is no serial correlation, the test statistic Q , from equation (3.13) follows a chi-squared distribution with m degrees of freedom χ_m^2 [5, 8]. Therefore, we can reject a value at risk model when $p = 1 - \chi_m^2(Q)$ becomes too small. However, the results from this test need to be interpreted with care since the Ljung-Box test has a low power when used on highly skewed binary data, as is typically the case when backtesting value at risk [25]. Moreover, the power of the Ljung-Box tests decreases when the number of lags m becomes too high. Therefore, we will test only for serial correlation, so we set the number of lags to $m = 1$. In this sense, the backtest from this section is similar to Christoffersen backtest [19], but as we will show in the next section, the test in this section is also extendable to expected shortfall.

Lastly, this independence test can be combined with a two-sided unconditional coverage test by using the sum of both statistics [7]. The Z -score from equation (3.12) is normally distributed, so that Z^2 has a chi-squared distribution with one degree of freedom χ_1^2 . This can be combined with the Ljung-Box statistic Q from equation (3.13), which also has a chi-squared distribution. When we test for only serial correlation, $m = 1$, the combined statistic $Z^2 + Q$ has a chi-squared distribution with 2 degrees of freedom. Therefore, a combined test could be defined using $p = 1 - \chi_2^2(Z^2 + Q)$.

3.3.2 Backtesting Expected Shortfall

Backtesting expected shortfall is slightly more intricate than backtesting value at risk. However, the general idea is the same. We start by defining an expected shortfall failure indicator, and then we check if the expected shortfall failure indicators satisfy the unconditional coverage property and the independence property. In this section

we follow Costanzino and Curran and define the expected shortfall failure indicator [49].

Definition 3.13 (ES Failure indicator). Let x_i , with $i = 1, \dots, N$, be the realized profit or loss at day i . Then, the expected shortfall failure indicator $H_{\text{ES}(\ell)}^{(i)}$ is given by

$$H_{\text{ES}(\ell)}^{(i)} = \frac{1}{\ell} \int_0^\ell \mathbb{1}_{\{-x_i \geq \text{VaR}_i(u)\}} du, \quad (3.14)$$

where $\mathbb{1}$ is used to denote the indicator function.

Note that we cannot determine the expected shortfall failure indicator $H_{\text{ES}(\ell)}^{(i)}$ solely from the corresponding expected shortfall $\text{ES}_i(\ell)$. Rather we need information from the profit and loss distribution in order to determine $H_{\text{ES}(\ell)}^{(i)}$. When the historical simulation method from Section 3.2.1 is used to estimate the profit and loss distribution, we can compute the failure indicator with

$$H_{\text{ES}(\ell)}^{(i)} = \sum_{i=1}^{\lfloor n\ell \rfloor} \frac{\mathbb{1}_{\{x_i \leq X(i)\}}}{\lfloor n\ell \rfloor}, \quad (3.15)$$

where n is the size of the calibration window used in the historical simulation.

Before we define the backtesting statistics for the expected shortfall, it is convenient to know the first two moments of the expected shortfall failure indicators $H_{\text{ES}(\ell)}^{(i)}$. Therefore, we will derive these before we continue to define the expected shortfall backtests.

Lemma 3.14. *The first two moments of the expected shortfall indicator $H_{\text{ES}(\ell)}^{(i)}$ are given by*

$$\mathbb{E}[H_{\text{ES}(\ell)}^{(i)}] = \ell/2, \quad \text{and} \quad \mathbb{E}[(H_{\text{ES}(\ell)}^{(i)})^2] = \ell/3. \quad (3.16)$$

Proof. First consider the mean of the expected shortfall failure indicator. Using Fubini's theorem, allows us to take the expectation inside the integral. The result then follows from the fact that the value at risk failure indicator is a Bernoulli random variable.

$$\begin{aligned} \mathbb{E}[H_{\text{ES}(\ell)}^{(i)}] &= \mathbb{E} \left[\frac{1}{\ell} \int_0^\ell \mathbb{1}_{\{-x_i \geq \text{VaR}_i(u)\}} du \right] \\ &= \frac{1}{\ell} \int_0^\ell \mathbb{E}[\mathbb{1}_{\{-x_i \geq \text{VaR}_i(u)\}}] du \\ &= \frac{1}{\ell} \int_0^\ell u du = \frac{\ell}{2}. \end{aligned}$$

Similarly, the second moment can be computed as follows.

$$\begin{aligned}
\mathbb{E}[(H_{\text{ES}(\ell)}^{(i)})^2] &= \mathbb{E}\left[\left(\frac{1}{\ell} \int_0^\ell \mathbb{1}_{\{-x_i \geq \text{VaR}_i(u)\}} du\right)^2\right] \\
&= \frac{1}{\ell^2} \mathbb{E}\left[\left(\int_0^\ell \mathbb{1}_{\{-x_i \geq \text{VaR}_i(u)\}} du\right)\left(\int_0^\ell \mathbb{1}_{\{-x_i \geq \text{VaR}_i(v)\}} dv\right)\right] \\
&= \frac{2}{\ell^2} \mathbb{E}\left[\int_0^\ell \int_0^v \mathbb{1}_{\{-x_i \geq \text{VaR}_i(u)\}} \mathbb{1}_{\{-x_i \geq \text{VaR}_i(v)\}} du dv\right] \\
&= \frac{2}{\ell^2} \int_0^\ell \int_0^v \mathbb{E}[\mathbb{1}_{\{-x_i \geq \text{VaR}_i(u)\}} \mathbb{1}_{\{-x_i \geq \text{VaR}_i(v)\}}] du dv \\
&= \frac{2}{\ell^2} \int_0^\ell \int_0^v u du dv = \frac{2}{\ell^2} \cdot \frac{\ell^3}{6} = \frac{\ell}{3}. \quad \square
\end{aligned}$$

3.3.2.1 Unconditional Coverage

The unconditional coverage test for expected shortfall is very similar to unconditional coverage test for value at risk. Hence, when the number of backtesting days N is large enough we can use a Z -test in order to check the correctness of a given expected shortfall model.

Theorem 3.15. *If the expected shortfall model is correct, the failure rate $H_{\text{ES}(\ell)}^{(i)}$ from Definition 3.13, is asymptotically normal with mean $\ell/2$ and variance $\ell(4 - 3\ell)/12$, and therefore, admits a Z -test, with Z -score given by*

$$Z = \sqrt{N} \frac{\left(\frac{1}{N} \sum_{i=1}^N H_{\text{ES}(\ell)}^{(i)}\right) - \ell/2}{\sqrt{\ell(4 - 3\ell)/12}}. \quad (3.17)$$

Proof. Under the assumption that the expected shortfall model is correct, it follows from Lemma 3.14 that all failure indicators $H_{\text{ES}(\ell)}^{(i)}$ have mean $\mathbb{E}[H_{\text{ES}(\ell)}^{(i)}] = \ell/2$ and variance $\mathbb{E}[(H_{\text{ES}(\ell)}^{(i)})^2] - \mathbb{E}[H_{\text{ES}(\ell)}^{(i)}]^2 = (\ell/3) - (\ell/2)^2 = \ell(4 - 3\ell)/12$. It then follows by the central limit theorem that

$$\sqrt{N} \frac{\left(\frac{1}{N} \sum_{i=1}^N H_{\text{ES}(\ell)}^{(i)}\right) - \ell/2}{\sqrt{\ell(4 - 3\ell)/12}} \xrightarrow[N \rightarrow \infty]{d} \mathcal{N}(0, 1).$$

Therefore, Z converges in distribution to a standard normal distribution. So, when the sample size N is large enough, we can use a standard Z -test. \square

Similar to the unconditional coverage test for value at risk, we can use to Z -score from equation (3.17) to define either a one-sided or two-sided Z -test though the p -value $p = \Phi(-Z)$ or $p = 2\Phi(-|Z|)$, respectively.

3.3.2.2 Independence

We can also extend the value at risk independence test from Section 3.3.1.2 in order to test an expected shortfall model. The Ljung-Box statistic that can be used to test an expected shortfall model is then defined as follows.

Definition 3.16 (Ljung-Box statistic). Let $H_{\text{ES}(\ell)}^{(i)}$ be the expected shortfall failure indicator, for $i = 1, \dots, N$, and let m be a number of lags. Then, the Ljung-Box test statistic is given by

$$Q = N(N + 2) \sum_{k=1}^m \frac{\rho_k^2}{N - k}, \quad (3.18)$$

where

$$\rho_k = \frac{\sum_{i=k+1}^N \left(H_{\text{ES}(\ell)}^{(i)} - \ell/2 \right) \left(H_{\text{ES}(\ell)}^{(i-k)} - \ell/2 \right)}{\sum_{i=1}^N \left(H_{\text{ES}(\ell)}^{(i)} - \ell/2 \right)^2}.$$

As in the value at risk independence test, when the expected shortfall failure indicators are indeed independent then the statistic Q , from equation (3.18), follows a chi-squared distribution with m degrees of freedom. Therefore, when $p = 1 - \chi_m^2(Q)$ is too small, we can reject the hypothesis that the failure indicators are independent and in extension reject the expected shortfall model. Although the Ljung-Box test is better suited to test expected shortfall since the failure indicators are continuous instead of binary, the power of this test is still relatively low, especially when used on a low significance level such as $\ell = 2.5\%$, as is typical when backtesting expected shortfall. Also, the power decreases when the number of lags is chosen too high. Therefore, we will also test for series correlation only and set the number of lags to $m = 1$.

Similar to the value at risk backtest, we can also define a combined test for independence and unconditional coverage of the expected shortfall. When $m = 1$, the combined statistic $Z^2 + Q$ has a chi-squared distribution with 2 degrees of freedom χ_2^2 , which allows us to reject an expected shortfall model when $p = 1 - \chi_2^2(Z^2 + Q)$ becomes sufficiently small.

Chapter 4

Risk Measurement for Interest Rate Options

When estimating the profit and loss distribution of a portfolio consisting of interest rate options, the relevant risk factors are the interest rates and implied volatilities. Hence, in a historical simulation framework the changes in both of those risk factors within the chosen risk horizon are used for simulating possible outcomes of the position. Once we have determined the profit and loss distribution, we can estimate the value at risk or expected shortfall.

It is up to the risk manager to determine the specific choice of risk factors that are used in the historical simulation. In this chapter, we present different combinations of risk factors that can be used for interest rate options. We first present the risk factors we will use for the interest rates. After that, we will present different methods of applying shocks to the implied volatilities.

4.1 Interest Rate Shocks

As explained in Section 2.4, the price of interest rate options is based on either the forward Libor or the forward swap rate. Therefore, it seems natural to use these forward rates as risk factors in the historical simulation. However, this can lead to inconsistency within the generated scenarios. Consider the forward swap rates $S_{1,2}(0)$, $S_{2,3}(0)$, and $S_{1,3}(0)$. As explained in Section 2.5, we can also compute the value of $S_{1,3}(0)$ from $S_{1,2}(0)$ and $S_{2,3}(0)$ by the bootstrapping method. However, applying historical shocks to $S_{1,3}(0)$ will not necessarily result in the same scenarios as applying historical shocks to $S_{1,2}(0)$ and $S_{2,3}(0)$ and using the bootstrapping method to determine $S_{1,3}(0)$. So if we applied shocks to $S_{1,2}(0)$, $S_{2,3}(0)$, and $S_{1,3}(0)$ we would have two different values for $S_{1,3}(0)$. Hence, applying shocks to the forward interest rates can result in inconsistent scenarios.

Therefore, we do not use the forward rates as risk factors. Rather we will use the spot Libor and spot swap rates at different tenors as risk factors. Then in each scenario, we will use the bootstrapping method from Section 2.5 to determine the relevant forward rates, where we will use linear interpolation when we don't have the spot interest rate of a certain tenor. The specific set of tenors that we use will depend on the portfolio. Therefore, we will specify the tenors that are used in every experiment.

4.2 Implied Volatility Shocks

While determining the risk factors for interest rates is quite straightforward, but the risk factor choice for the implied volatilities is more intricate. As we have seen in Section 2.4.3, we typically do not have a single implied volatility. Rather, we need a different implied volatility for each strike in order to correctly recover market prices. This relation between strike and implied volatility is often referred to as the volatility smile.

Generally, the level of the volatility smile is based on the implied volatility of the at-the-money strike and provides a handle on fluctuations of option prices on a large scale. However, when the shape of the volatility smile changes, the change in implied volatility of an away-from-the-money option can be lower or higher than the corresponding change at-the-money. Therefore, a historical simulation method that only considers changes in the level of the volatility smile can generate either too optimistic or too pessimistic forecasts, especially for options whose strike is far from the at-the-money strike. On the other hand, the level of the volatility smile accounts for most of the variation which might be enough to determine accurate forecasts.

Furthermore, it is not clear which implied volatility we should use as risk factors. We could use either the normal implied volatility from Bachelier's model or the Black implied volatility from Black's model. Yet another possibility is to use the parameters of the SABR model as risk factors. However, due to the negative interest rates currently observable in the European interest rate market, we cannot use the Black implied volatility or the SABR parameters directly. Instead, we need to use the shifted Black implied volatility or the parameters of the shifted SABR model in order to handle negative interest rates. Which of these approaches will give the most accurate forecasts of the profit and loss distribution, will be determined in the next chapter by comparing their results on several test portfolios.

In this section, we first describe how the Black's implied volatility can be used as risk factors in a historical simulation. Then, we adapt this method and show how we can achieve a similar result using the normal implied volatility from Bachelier's model. Lastly, we also show how the parameters of the SABR model can serve as

risk factors. For each of these approaches, we describe a method where only the level of the volatility smile is allowed to vary and a method where we model changes in both the level and the shape of the volatility smile.

4.2.1 Using Black's Model

In this section, we present two methods of using the implied volatility from Black's model as risk factors to model changes in both level and shape of the volatility smile. The first method we describe was proposed by Malz [16, 22]. Secondly, we propose a new method that can also be used to model the changes in level and shape of the volatility smile. Using a small approximation, we are able to derive closed form formula for the risk factors, which makes our method much faster than the method of Malz.

4.2.1.1 Malz's Method

Malz proposed a method to model both changes in level and shape of the volatility smile by applying historical shocks to implied volatilities at different strikes [16, 22]. In this thesis, we will slightly adapt Malz's method by using the shifted Black implied volatility $\sigma_B^{s_B}$, enabling that this method can also be applied when interest rates are negative. We will apply shocks to the shifted Black implied volatilities $\sigma_B^{s_B}$, where the shift s has to be fixed throughout the historical simulation.

The main drawback of Malz's method is that it is unclear which strikes should be used. We could use three fixed strikes during the whole historical simulation or we could use three strikes relative to the prevailing forward rate. In this section, we describe the latter option and will use relative strikes. To define these relative strikes, we will use the shifted log-moneyness from Definition 2.21. We will then use the strikes that correspond to the moneyness values $M_- = -0.25$, $M_{ATM} = 0$, and $M_+ = 0.25$. We will use the implied volatilities at the strikes

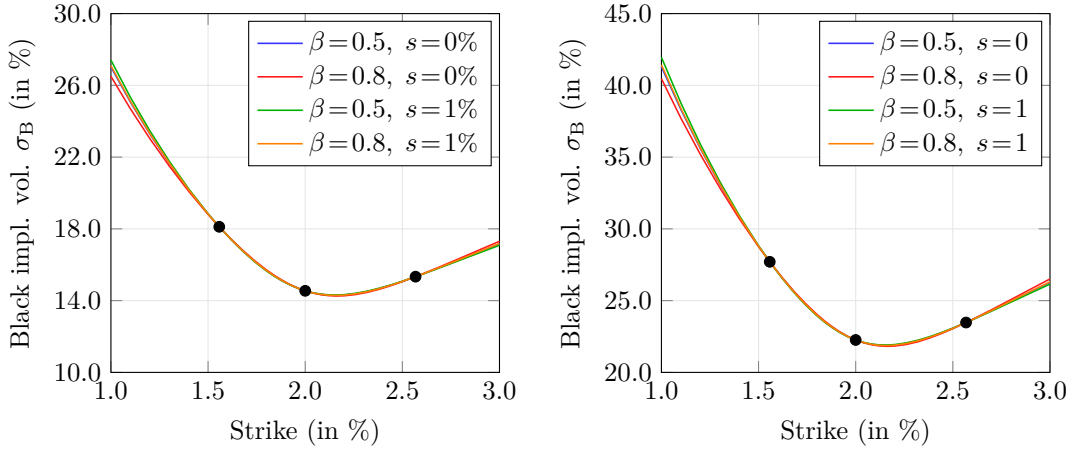
$$K = (F_0 + s_B) \exp(M) - s_B, \quad \text{for } M = M_-, M_{ATM}, M_+, \quad (4.1)$$

as risk factors in the historical simulation. Note that M_{ATM} corresponds to the at-the-money strike $K = F_0$ and that $K_- < F_0 < K_+$. Assuming that we have historical data that contains the SABR parameters each day, we can simply use Theorem 2.28 to compute the implied volatilities needed in this method.

From a historical simulation perspective, we will use the shifted Black implied volatility at the strikes corresponding to M_- , M_{ATM} , and M_+ as risk factors. To ensure that these implied volatilities remain positive in every scenario, we use relative shocks as in equation (3.7).

To price a given portfolio in each scenario, we typically need implied volatilities for strikes that do not coincide with M_- , M_{ATM} , and M_+ . In order to determine the implied volatility at all strikes, we can calibrate a SABR model using the three implied volatilities in the scenario. We can then use the SABR formula from Theorem 2.28 to compute the implied volatilities for the strikes we need. However, this means that we have to run a numerical calibration algorithm in every scenario for every interest rate option in our portfolio. For large portfolios, this can quickly become unmanageable and therefore makes this method less suitable in large scale historical simulation.

When the SABR model is calibrated in a scenario, it does not matter which values we choose for β and s . This can be seen in Figure 4.1, where we calibrated the shifted SABR model to three implied volatilities using different β and s .



(a) Volatility smiles for maturity $T = 1$.

(b) Volatility smiles for maturity $T = 20$.

Figure 4.1: Calibration of the SABR model with different values β and s , using three shifted Black implied volatilities $\sigma_B^{s_B}$, with $s_B = 0$, at M_- , M_{ATM} , and M_+ , indicated by the black circles. The forward rate is $F_0 = 2\%$.

4.2.1.2 Level, Slope, and Curvature Method

Instead of using the implied volatilities at three strikes, the idea is to use the at-the-money shifted Black implied volatility, slope and curvature to capture the shape of the volatility smile. We can obtain the slope and curvature by differentiating the SABR formula from Theorem 2.28 once and twice, respectively. However, this would lead to a system of trivariate polynomials of degree 3 and 4. To invert such a system, we would have to resort to numerical methods which has the same drawback as Malz's method, in that it is too slow to be used in a large scale historical simulation. Instead, we can use an approximate version of Theorem 2.28 that still captures the shape of the volatility smile around the at-the-money strike accurately.

The approximation we use in this thesis is similar to the one used by Le Floc'h and Kennedy [46] and is obtained by setting the maturity $T = 0$. This is generally a good approximation, since the contribution of the maturity term is typically small and can therefore be approximated by zero. This leads to a simplified expression for the shifted Black implied volatility

$$\sigma_B^{s_B}(F_0, K, T; \alpha, \rho, \nu, \beta, s) = \frac{\nu \log((F_0 + s_B)/(K + s_B))}{\log\left(\frac{\sqrt{1-2\rho z+z^2+z-\rho}}{1-\rho}\right)}, \quad (4.2)$$

where

$$z = \begin{cases} \frac{\nu (F_0 + s)^{1-\beta} - (K + s)^{1-\beta}}{\alpha (1-\beta)} & \text{if } \beta < 1, \\ \frac{\nu}{\alpha} \log((F_0 + s)/(K + s)) & \text{if } \beta = 1. \end{cases}$$

From equation (4.2), we can easily obtain the level L_B , slope S_B , and curvature C_B . Note that we differentiate with respect to the shifted log-moneyness from Definition 2.21 to capture the level, slope, and curvature relative to the forward rate. This gives

$$\begin{aligned} L_B &= \lim_{K \rightarrow F_0} \sigma_B^{s_B} = \alpha \frac{(F_0 + s_B)^\beta}{F_0 + s_B}, \\ S_B &= \lim_{K \rightarrow F_0} \frac{\partial \sigma_B^{s_B}}{\partial M} = \frac{1}{2} \left(L_B \left(\beta \frac{F_0 + s_B}{F_0 + s} - 1 \right) + \nu \rho \right), \\ C_B &= \lim_{K \rightarrow F_0} \frac{\partial^2 \sigma_B^{s_B}}{\partial M^2} = \frac{1}{6} \left(L_B \left(\beta(\beta - 2) \left(\frac{F_0 + s_B}{F_0 + s} \right)^2 + 1 \right) + \frac{2 - 3\rho^2}{L_B} \nu^2 \right), \end{aligned} \quad (4.3)$$

where $M = M(F_0, K) = \log((K + s_B)/(F_0 + s_B))$ is the shifted log-moneyness from Definition 2.21.

This system of equations (4.3) can be solved analytically to find values α , ρ , and ν that correspond to a certain level L_B , slope S_B , and curvature C_B . With $s = s_B$ we find

$$\begin{aligned} \alpha &= L_B (F_0 + s_B)^{1-\beta}, \\ \nu &= \sqrt{\left((\beta - 1)L_B - 3S_B \right)^2 + 3(L_B C_B - S_B^2)}, \\ \rho &= \frac{2S_B + (1 - \beta)L_B}{\nu}. \end{aligned} \quad (4.4)$$

When using equation (4.4), it could happen that $\nu^2 < 0$, which is clearly invalid. In this case, we follow Le Floc'h and Kennedy [46] and force $\rho \in \{-1, 1\}$, depending on the sign of $2S_B + (1 - \beta)L_B$. That is, we set $\rho = \text{sgn}(2S_B + (1 - \beta)L_B)$. The value of ν is then recomputed using $\nu = (2S_B + (1 - \beta)L_B) / \rho$.

The idea is to use the level L_B , slope S_B , and curvature C_B from equation (4.3) as risk factors in a historical simulation. So for each day in the calibration window, we compute the values of L_B , S_B , and C_B using the SABR parameters from that day using a predetermined shift s_B . Next, we apply historical shocks to obtain the values of L_B , S_B , and C_B in each scenario. The complete volatility smile can then be recovered using equation (4.4) with $s = s_B$ and any $\beta \in [0, 1]$. Because the level L_B is the implied volatility for the at-the-money strike and as such should always be positive we will use relative shocks to ensure that the level L_B remains positive in each scenario. For the slope S_B and curvature C_B we don't have to use relative shocks since both are allowed to become negative.

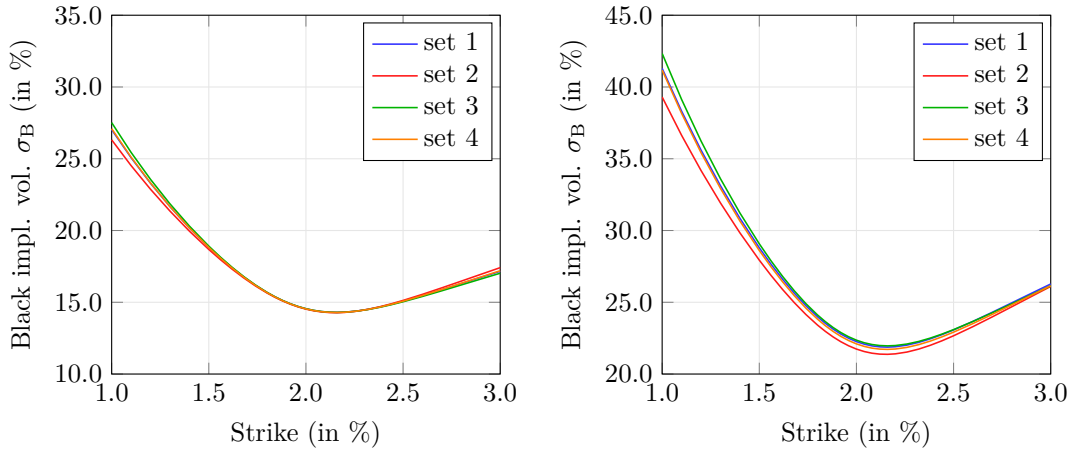
Note that the level L_B , slope S_B , and curvature C_B always have approximately the same value independent of the β and s that were used to calibrate the SABR model, but they still depend on the Black implied volatility shift s_B . So the choice of s_B will affect the value of the risk factors L_B , S_B , and C_B , which in turn will have an impact on the historical simulation. In Section 5.3.1 of the next chapter, we will investigate the effect of using different values for the shift s_B and determine which shift gives the most accurate results.

To show that the volatility smile obtained from a given level L_B , slope S_B , and curvature C_B are indeed independent of the chosen values for β and s , we use the method in this section to obtain SABR parameters with different values of β and s . In Figure 4.2, we show the resulting volatility smiles, where the parameters from set 2, 3, and 4 are obtained by recalibrating them from the parameters of set 1 in Table 4.1. As expected, this method yields more accurate results for the smaller maturity since the approximation from equation (4.2) is better when the maturity is small. Nonetheless, even for the large maturity we find that the results remain adequate.

Table 4.1: Analytic recalibration of the shifted Black implied volatility smile.

set	β	s	α	ρ	ν
1	0.5	0.0%	0.0200	-0.1000	0.6000
2	0.8	0.0%	0.0647	-0.1678	0.6103
3	0.5	1.0%	0.0163	-0.0614	0.5937
4	0.8	1.0%	0.0468	-0.1082	0.5980

Effect of using different β and s when recovering SABR parameters α , ρ , and ν from the level L_B , slope S_B , and curvature C_B . The parameters from set 2, 3, and 4 are obtained by recalibrating them from the parameters of set 1 with a forward rate $F_0 = 2\%$, using the method described in this section.



(a) Volatility smiles for maturity $T = 1$. (b) Volatility smiles for maturity $T = 20$.

Figure 4.2: Effect of using different β and s when recovering SABR parameters α , ρ , and ν from the level L_B , slope S_B , and curvature C_B . The resulting shifted Black implied volatilities $\sigma_B^{s_B}$, with $s_B = 0$, are shown for different maturities using the parameters in Table 4.1

Instead of modeling changes in both the level and shape of the volatility smile, we can alternatively model only the changes in the level of the volatility smile. This can be accomplished using only the level L_B as a risk factor. Then, in each scenario we can use the today values of S_B and C_B in order to recover the SABR parameters α , ρ , and ν using equation (4.4). Since most of the variation is typically accounted for by vertical movements of the volatility smile, using only the L_B could be a reasonable approximation.

4.2.2 Using Bachelier's Model

In the previous section, we showed how the shifted Black implied volatility $\sigma_B^{s_B}$ can be used as risk factors in a historical simulation. Another possibility is to use the normal implied volatility from Bachelier's model. In this section, we will show how Malz's method can be used with normal implied volatilities. After that, we also show how to determine the level, slope, and curvature of the normal implied volatility smile.

4.2.2.1 Malz's Method

Malz's method can also be applied to the normal implied volatility. However, when using normal implied volatility, it makes sense to also use the simple moneyness from Definition 2.24 to define the strikes at which we applied the historical shocks.

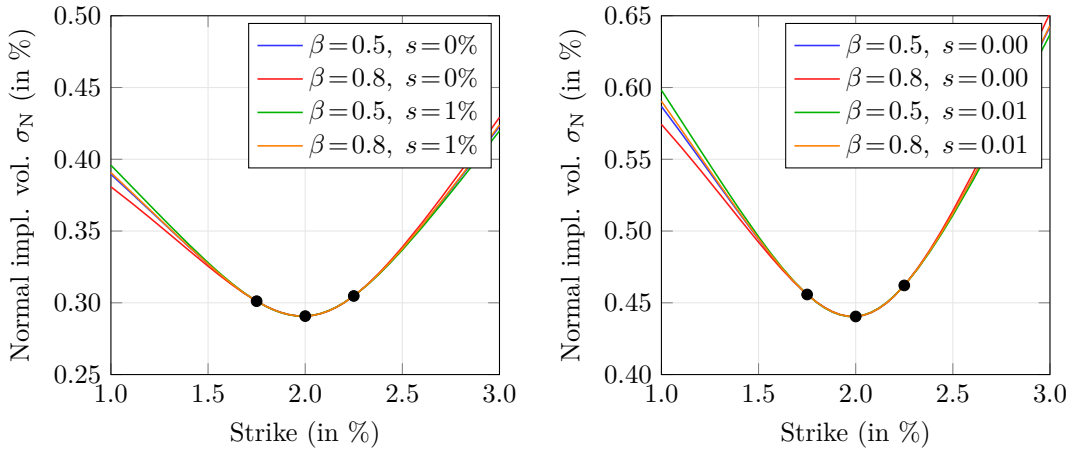
Because of this, we will also need to revisit the moneyness values that are used. Here, we will use the values $M_- = -0.0025$, $M_{\text{ATM}} = 0$, and $M_+ = 0.0025$, so we use the strikes given by

$$K = M + F_0, \quad \text{for } M = M_-, M_{\text{ATM}}, M_+. \quad (4.5)$$

So, in this case we will use the normal implied volatilities corresponding to the strikes K_- , $F_0 = K_{\text{ATM}}$, and K_+ as risk factors in the historical simulation. Assuming that we have historical data containing the SABR parameters each day, we can use Theorem 2.27 to compute the implied volatilities at these strikes.

With this method, the risk factors are three implied volatilities, which should always be positive. To ensure this, we apply a log-transformation as with did in the previous sections. Then, in every scenario, the complete volatility smile can be recovered by calibrating a SABR model to the three implied volatilities.

When the SABR model is calibrated in a scenario, it does not matter which values we use for β and s . This can be seen in Figure 4.3, where we calibrated the shifted SABR model to three implied volatilities using different combinations of β and s .



(a) Volatility smiles for maturity $T = 1$.

(b) Volatility smiles for maturity $T = 20$.

Figure 4.3: Calibration of the SABR model with different values β and s , using three normal implied volatilities σ_N , at M_- , M_{ATM} , and M_+ , indicated by the black circles. The forward rate is $F_0 = 2\%$.

4.2.2.2 Level, Slope, and Curvature Method

We can also adapt the method from Section 4.2.1.2 to use the normal implied volatility from Theorem 2.27. We would then model the level, slope, and curvature of the normal implied volatility smile. To proceed, we first make an approximation

to Theorem 2.27 similar to what we have done in the previous section.

$$\sigma_N(F_0, K, T; \alpha, \rho, \nu, \beta, s) = \frac{\nu(F_0 - K)}{\log\left(\frac{\sqrt{1-2\rho z+z^2+z-\rho}}{1-\rho}\right)}, \quad (4.6)$$

where

$$z = \begin{cases} \frac{\nu(F_0 + s)^{1-\beta} - (K + s)^{1-\beta}}{\alpha(1-\beta)} & \text{if } \beta < 1, \\ \frac{\nu}{\alpha} \log((F_0 + s)/(K + s)) & \text{if } \beta = 1. \end{cases}$$

Then, from equation (4.6) we can easily obtain the level L_N , slope S_N , and curvature C_N of the at-the-money normal implied volatility. Note that we differentiate with respect to the simple moneyness from Definition 2.24 instead of the shifted log-moneyness from the previous section. The level L_N , slope S_N , and curvature C_N are then given by

$$\begin{aligned} L_N &= \lim_{K \rightarrow F_0} \sigma_N = \alpha(F_0 + s)^\beta, \\ S_N &= \lim_{K \rightarrow F_0} \frac{\partial \sigma_N^{s^2}}{\partial M} = \frac{1}{2} \left(L_N \frac{\beta}{F_0 + s} + \nu \rho \right), \\ C_N &= \lim_{K \rightarrow F_0} \frac{\partial^2 \sigma_N^{s^2}}{\partial M^2} = \frac{1}{6} \left(L_N \frac{\beta(\beta-2)}{(F_0 + s)^2} + \frac{2-3\rho^2}{L_N} \nu^2 \right), \end{aligned} \quad (4.7)$$

where $M = M(F_0, K) = K - F_0$ is the simple moneyness.

We are also able to analytically invert this system to find values α , ρ , and ν that correspond to a certain level L_N , slope S_N , and curvature C_N . This gives

$$\begin{aligned} \alpha &= \frac{L_N}{(F_0 + s)^\beta}, \\ \nu &= \frac{\sqrt{(L_N \beta - 3(F_0 + s) S_N)^2 + L_N^2 \beta + 3(F_0 + s)^2 (L_N C_N - S_N^2)}}{F_0 + s}, \\ \rho &= \frac{2 S_N - L_N \beta / (F_0 + s)}{\nu}. \end{aligned} \quad (4.8)$$

As in the previous section, it can happen that if we use (4.8) we get $\nu^2 < 0$. In those cases, we set $\rho = \text{sgn}(2 S_N - L_N \beta / (F_0 + s))$ and recompute the value of ν with $\nu = (2 S_N - L_N \beta / (F_0 + s)) / \rho$.

From a historical simulation perspective, we could also use L_N , S_N , and C_N from equation (4.7) as risk factors. Note that since L_N is actually the at-the-money implied volatility it has to be positive so we apply relative shocks as we did to L_B in the previous section.

Note that, as in the previous section, the level L_N , slope S_N , and curvature C_N will have approximately the same value, regardless of the β and s that are used in the calibration of the SABR model. So, the L_N , S_N , and C_N are independent of the chosen β and s . To show this, we use the method in this section to obtain SABR parameters with different values of β and s . In Figure 4.4, we show the resulting volatility smiles, where the parameters from set 2, 3, and 4 are obtained by recalibrating them from the parameters of set 1 in Table 4.2. As expected, the results are more accurate for smaller maturity, since the approximation from equation (4.6) is better when the maturity is small. Moreover, the parameters from Table 4.2 are exactly the same as the parameters in Table 4.1 from the previous section. So, although L_N , S_N , and C_N are different from L_B , S_B , and C_B , we conclude that both methods are equally good in recovering the SABR model parameters.

Table 4.2: Analytic recalibration of the normal implied volatility smile.

set	β	s	α	ρ	ν
1	0.5	0.0%	0.0200	-0.1000	0.6000
2	0.8	0.0%	0.0647	-0.1678	0.6103
3	0.5	1.0%	0.0163	-0.0614	0.5937
4	0.8	1.0%	0.0468	-0.1082	0.5980

Effect of using different β and s when recovering SABR parameters α , ρ , and ν from the level L_N , slope S_N , and curvature C_N . The parameters from set 2, 3, and 4 are obtained by recalibrating them from the parameters of set 1 with a forward rate $F_0 = 2\%$, using the method described in this section.

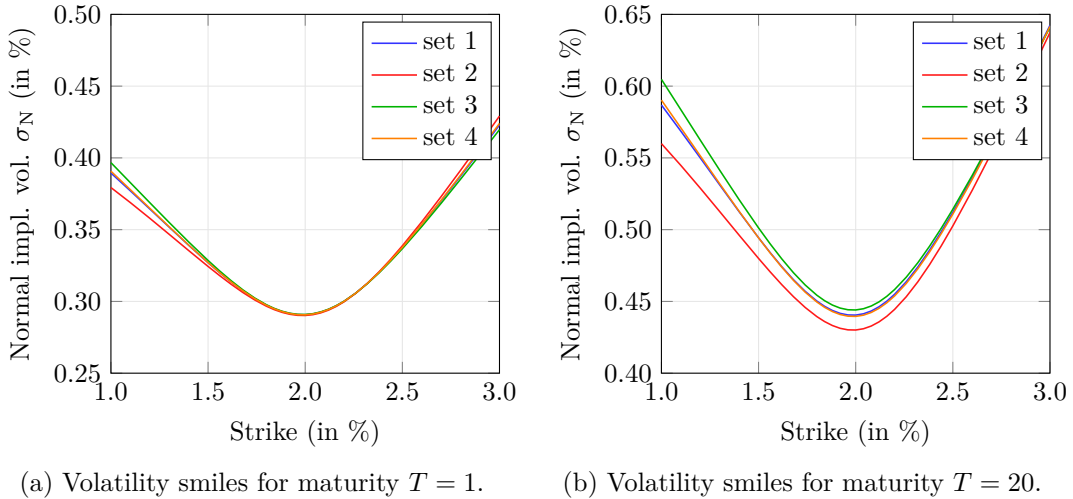


Figure 4.4: Effect of using different β and s when recovering SABR parameters α , ρ , and ν from the level L_N , slope S_N , and curvature C_N . The resulting normal implied volatilities σ_N are shown for different maturities using the parameters are in Table 4.2.

4.2.3 Using the SABR Model

Instead of using an implied volatility as in the previous sections, we can also use the parameters of the SABR model as risk factors directly. However, when using the SABR parameters as risk factors in a historical simulation, we need to be careful as not all parameters have a direct effect on the volatility smile and some of the parameters have an interaction with each other.

As explained in Section 2.4.3, the parameters $\beta \in [0, 1]$ and $s \geq 0$ are partially redundant. Because of this redundancy, these parameters are typically fixed before calibration and often the same values are used multiple months in a row. As these parameters rarely change they are not suitable to use in a historical simulation. Therefore, we will only consider the parameters α , ρ , and ν as risk factors.

Although the volatility smiles that can be obtained using different β and s are practically the same, the values for α , ρ and ν change when using different β or s . Hence, parameters that are obtained using a certain β, s -pair are not comparable with the parameters obtained using different β and s . So, to perform a historical simulation using the SABR parameters α , ρ , and ν we need to first recalibrate these parameters to the same β and s . To this end, we could use the analytical recalibration method we developed in Sections 4.2.2.2 or 4.2.1.2. Which choice of β and s that gives the most accurate results will be determined in Section 5.3.2 of the next chapter.

Assuming that all SABR parameters are obtained (or recalibrated) with the same β and s , it remains questionable if we can use SABR parameters as risk factors directly, because there is still some interaction between the parameters. For example, as ν tends to zero, the value of ρ becomes less important to the shape of the resulting volatility smile. Therefore, a historical shock to ρ obtained when the value of ν was large might not be representative if today's value of ν is small. Although the original SABR parameters have a well defined mathematical meaning, Moni notes that it is $\rho\nu$ that affects the slope of the volatility smile [47, 41]. Moreover, the smile curvature is linked to the way the volatility moves independently from the underlying. This gives the following reparameterization of the SABR model, that can be used as risk factors in a historical simulation.

$$\alpha, \quad \eta = \rho\nu, \quad \gamma = \nu\sqrt{1 - \rho^2}. \quad (4.9)$$

To obtain the original SABR parameters from these, we can use

$$\nu = \sqrt{\eta^2 + \gamma^2}, \quad \rho = \eta/\nu. \quad (4.10)$$

To use the SABR model, we need that $\alpha, \nu > 0$ and $\rho \in (0, 1)$. Therefore, we require that $\alpha, \gamma > 0$ and $\eta \in \mathbb{R}$. To ensure that α and γ remain positive after applying historical shocks, we will use relative shocks for these two parameter and use absolute shocks for the η parameter.

Instead of modeling changes in both the level and shape of the volatility smile, we can alternatively model only the changes in the level of the volatility smile. This can be done by considering only α as a risk factor. That is, we apply shocks to the α parameter and instead of applying shocks to η and γ we use their current values. When only using the α parameter as risk factor, the volatility smile can move vertically up and down, but since η and γ , or equivalently ρ and ν , remain fixed the shape of the volatility smile will also remain the same. Since most of the variation is typically accounted for by vertical movements of the volatility smile, using only the α parameter could be a reasonable approximation.

4.3 Summary

In this chapter, we have seen different methods that can be used to do a historical simulation for interest rate options. Each of these methods consists of a combination of risk factors for interest rates and implied volatilities. For interest rates, using the forward interest rate as risk factors can lead to inconsistent market scenarios. So, in order to generate realistic scenarios, it is necessary to use the spot interest rates at several different tenors.

Determining the risk factors to use for the implied volatilities is more complex. In this chapter, we obtained the risk factors based on parameterizations from three different models. With each of these methods, we can model changes in level and shape of the volatility smile, or we can model only the changes in level which can be slightly less accurate but also simpler since we have less risk factors. This leads to six different methods of generating implied volatility scenarios presented below.

- Methods from Section 4.2.1.2 based on Black's model.
 - Smile method: using the risk factors $\log(L_B)$, S_B , and C_B , we model changes in the level, slope and curvature of the volatility smile.
 - Level method: using the risk factor $\log(L_B)$, we model changes in the level of the volatility smile only.
- Methods from Section 4.2.2.2 based on Bachelier's model.
 - Smile method: using the risk factors $\log(L_N)$, S_N , and C_N , we model changes in the level, slope and curvature of the volatility smile.
 - Level method: using the risk factor $\log(L_N)$, we model changes in the level of the volatility smile only.

- Methods from Section 4.2.3 based on the SABR model.
 - Smile method: using the risk factors $\log(\alpha)$, η , and $\log(\gamma)$, we model changes in the level, slope and curvature of the volatility smile.
 - Level method: using the risk factor $\log(\alpha)$, we model changes in the level of the volatility smile only.

By combining the risk factors for interest rates, i.e. the spot interest rates, with the risk factors for implied volatility, we obtain six different historical simulation methods. However, the methods based on Black's model and the methods based on the SABR model have free parameters. For the method based on Black's model, the shift s_B needs to be chosen. For the methods based on the SABR model, we need to select which β and s we use to recalibrate each observation, before applying the historical shocks.

Chapter 5

Empirical Study and Results

In this chapter, we test the historical simulation methods from the previous chapter on market data to assess which method gives the most accurate forecast of the value at risk and expected shortfall. By testing on market data, we can determine which method gives the most accurate results in practice. We start this chapter with a description of the market data that we used. Then, we describe the portfolio used in each of the backtests. Lastly, we will present the results obtained in each of the backtests.

5.1 Market Data

The data used in this thesis consists of all the data necessary to price swaptions of different maturities and tenors. As such, the data consists of daily observations of both the interest rates and the implied volatilities. In total, our dataset contains 1300 daily observations starting from 20-05-2010 and ending at 19-06-2015. All data were provided by Rabobank, based on several different data sources.

The interest rate data is provided as Euribor spot swap rates with different maturities up to 40 years. As explained in Section 4.1, these spot rates can be used directly in a historical simulation. However, in order to price a swaption, we need the forward rate and an annuity factor. These can be obtained by the bootstrapping method from Section 2.5.

The implied volatilities are provided as SABR model parameters. That is, for each combination of maturity and tenor, we have daily observations of the SABR parameters α , ρ , ν , β , and s . These parameters are typically obtained by calibrating the SABR model to available market implied volatilities. Since we are provided with these parameters directly, we can skip the calibration process required by our historical simulation methods and use the SABR model parameters directly. How

the parameters are used depends on the method we employ to generate the historical scenarios described in Section 4.2.

A particularly interesting feature of our dataset can be seen in Figure 5.1. The 1×1 forward swap rate becomes negative in the last part of the data. This is interesting because it allows us to see how well the methods from Chapter 4 actually perform in a market with negative interest rates. Moreover, it highlights the need for the models we developed, as the conventional methods used in practice are unable to cope with negative interest rates and would thus be unable to estimate the value at risk or expected shortfall.

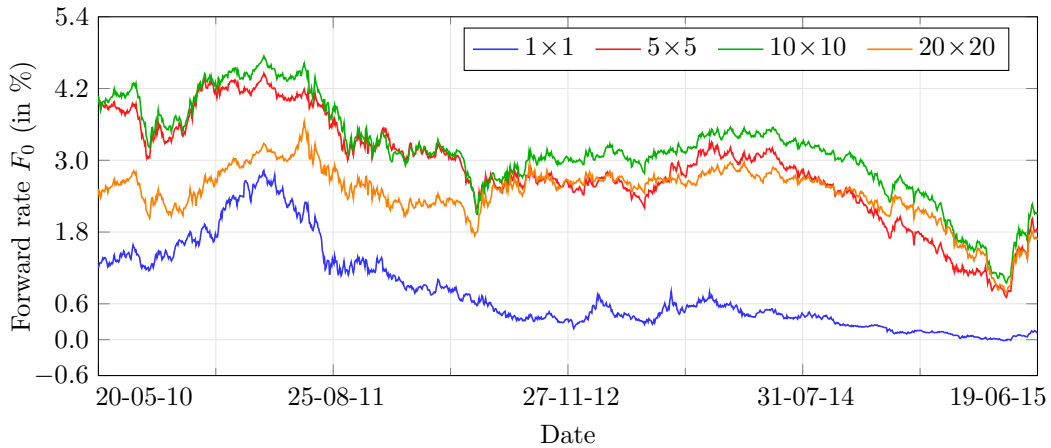


Figure 5.1: Forward swap rates for different combinations of maturity \times tenor.

5.2 Test Portfolio

In order to test the performance of each historical simulation method, we need a test portfolio. In this thesis, we will only use payer swaptions, but the same test could be applied to other types of options as well. A test portfolio needs to be large enough, so that the correlations between the different products will have an effect on the resulting value at risk or expected shortfall. We also want to have swaptions across a range of different strikes to better capture the effect of changes in the implied volatility smile. On the other hand, our backtest requires us to compute the value at risk or expected shortfall 1000 times using each method. Therefore, we need the test portfolio to be small enough such that the value at risk or expected shortfall can be computed quickly.

In this thesis, we will use a portfolio consisting of payer swaptions across 16 different combinations of maturities and tenors. For each maturity-tenor pair, the portfolio contains 3 swaptions, each with a different strike. So in total, our test portfolio

contains 48 swaptions with different combinations of maturities, tenors and strikes. For the maturities and tenors, we use every combination of 1, 5, 10, and 20 years. The strikes of the swaptions depend on the prevailing forward swap rate and the maturity of the swaption. For each maturity and tenor, the test portfolio contains one in-the-money, one at-the-money, and one out-of-the-money swaption with the following strikes

$$F_0 - 0.001\sqrt{T}, \quad F_0, \quad F_0 + 0.001\sqrt{T},$$

where F_0 denotes the forward rate at the day the portfolio is constructed and T the maturity of the swaption.

Example 5.1. The 1×1 forward swap rate on 19-06-15 is approximately 0.12%. Therefore, the swaptions with maturity and tenor equal to 1 in our test portfolio will have the strikes: 0.02%, 0.12%, and 0.22%, corresponding to an in-the-money, an at-the-money, and an out-of-the-money swaption respectively. \triangle

Instead of buying each of the swaptions as described above, we can also sell them, resulting in a second portfolio which has opposite value compared to the original portfolio. By looking at both portfolios simultaneously, we effectively test both sides of the profit and loss distribution. Therefore, we will use both these portfolios in the subsequent backtests. The portfolio obtained by buying each swaption will be referred to as the long portfolio and the portfolio where each swaption is sold will be called the short portfolio.

Remark 5.2. The choice of test portfolio does have an influence on the results presented in the next section. However, we repeated all the backtests using several other test portfolios. Although the resulting p -values of these backtests are different, the overall conclusions remain largely the same. Therefore, we only present the results using the portfolio as described above. \triangle

5.3 Backtests

In this section, we will present the results of our backtests. We started by comparing the methods based on Black's model by doing multiple backtests with various values for the Black model shift s_B . Then, we continued with a similar comparison for the SABR model based methods, where we also perform backtests for several different combinations of β and s . Lastly, we tested each method from Chapter 4 to find out which one of them gives to most accurate estimation of the value at risk and expected shortfall.

Following the standards set by the Basel Committee on Banking Supervision, all backtests in this section were based on the estimates of the VaR(1%) and the

ES(2.5%). The calibration window is set to 250 trading days, which is approximately one year [29, 48]. Although the Basel Committee on Banking Supervision requires the use of a 10 day risk horizon, a report by McKinsey finds that most banks are using a 1 day risk horizon to estimate the value at risk or expected shortfall and then scale the result to obtain an estimate for the 10 day risk horizon [42]. Therefore, we also used a 1 day risk horizon for our historical simulation. By moving the calibration window, this allowed us to generate 1000 estimates for the value at risk and expected shortfall. Then, for each of these 1000 samples, we also computed the realized profit or loss by using the data of the next day. In this way, we were able to compare each value at risk or expected shortfall estimate to the realized losses. These data can then be used to compute the backtest statistics as described in Section 3.3.

5.3.1 Effect of s_B in Black's Model Based Methods

In Section 4.2.1, we have described two historical simulation methods based on Black's model, one is based on shocking only the level of the volatility smile whereas the other also shocks the slope and curvature of the volatility smile. These methods still have one free parameter, namely the Black's model shift s_B . In this section, we will investigate which shift value gives the most accurate historical simulation. To this end, we perform backtests with both the level and the smile method using different values of the shift parameter s_B .

As can be seen in Table 5.1, all p values in the value at risk backtesting results are larger than 50%. Based on these results we cannot reject the use of any shift s_B and it is not possible to distinguish between the Black's model based methods that use a different shift. The reason that most p -values are the same is due to the fact that value at risk backtesting is based on the total number of times the value at risk is exceeded. With a significance level of $\ell = 1\%$ we expect around 10 breaches in our samples of 1000 value at risk estimates. The backtest results from Table 5.1 have between 8 and 12 breaches. Since this backtest is symmetric, 8 or 12 breaches correspond to a p -value of 52.50%, 9 or 11 breaches yield a p -value of 75.06%, and 10 breaches is precisely the expected value resulting in a p -value of 100%.

On the other hand, the expected shortfall backtesting results from Table 5.2 show more variation. This is because the backtest of expected shortfall do not only consider the number of breaches but also recognize the size of each breach. This results in more possible outcomes and, hence, more variation of the p -values. Moreover, it can be seen that the p -values decrease by increasing the shift. For a shift of 3% we can even reject both the level and the smile methods at the 5% significance level, based on the results of the short portfolio. This provides clear evidence that higher values of the shift s_B decreases the accuracy of both Black's model based methods.

Since these conclusions hold only in the backtests of the expected shortfall, we conclude that methods which correctly estimate the value at risk do not necessarily need to give accurate estimates of the expected shortfall. A possible reason for this could be that estimating value at risk requires a correct forecast of the profit and loss distribution up to the ℓ th quantile, whereas estimating the expected shortfall requires the complete tail of the profit and loss distribution to give accurate estimates.

This also indicates that, on average, the shifted Black implied volatility σ_B is more accurate than the normal implied volatility σ_N of Bachelier's model. To see this, consider the approximation $\sigma_N \approx \sigma_B^{s_B}(F_0 + s_B)$ [40]. When the shift s_B increases it starts to dominate the forward rate F_0 , and the term $F_0 + s_B$ will be almost equal to s_B . So for a large shift s_B , the shifted Black implied volatility $\sigma_B^{s_B}$ and the normal implied volatility σ_N are approximately equal up to the constant factor. This phenomenon will be further investigated in Section 5.3.3, where we compare the methods based on Black's model with the methods based on Bachelier's model.

Because the shift parameter s_B needs to be at least 1% in order to price every product in our test portfolios we will continue with the lowest shift possible and use the shift $s_B = 1\%$ in the subsequent sections.

Table 5.1: Value at risk backtest results.

s_B	Level		Smile	
	Long	Short	Long	Short
1.0%	75.06%	75.06%	75.06%	75.06%
2.0%	100.00%	52.50%	100.00%	75.06%
3.0%	100.00%	52.50%	100.00%	75.06%

The p -values from the unconditional coverage backtest from Section 3.3.1.1. The backtests are performed using the level and smile methods from Section 4.2.1 on both the long and the short portfolio with a significance level $\ell = 1\%$.

Table 5.2: Expected shortfall backtest results.

s_B	Level		Smile	
	Long	Short	Long	Short
1.0%	35.11%	10.27%	26.81%	11.56%
2.0%	32.18%	7.08%	24.37%	5.44%
3.0%	38.20%	4.14%	26.81%	4.75%

The p -values from the unconditional coverage backtest from Section 3.3.2.1. The backtests are performed using the level and smile methods from Section 4.2.1 on both the long and the short portfolio with a significance level $\ell = 2.5\%$.

5.3.2 Effect of β and s in SABR Model Based Methods

As with the methods based on Black’s model, the methods based on the SABR model also have free parameters. For the SABR based methods these are the β and the shift s . To check which combination of these parameters gives to most accurate value at risk and expected shortfall estimates we do a backtest with different values for these parameters.

As can be seen in Table 5.3, the value at risk backtesting results are inconclusive and we are not able to reject usage of any β and s combination. Nevertheless, these results show weak evidence that a shift of $s = 1.0\%$ yields the most accurate method, as we see most of the p -values decreasing when the shift increases.

The expected shortfall backtesting results from Table 5.4 do not provide more distinction either. To gain more insight in the ‘optimal’ choice of β and s a more extensive study is required. For the remainder of this thesis we will use $\beta = 0.2$ and $s = 1\%$ to compare the SABR model based methods to the methods based on different models. We choose these values because they provide accurate estimates of both the value at risk and the expected shortfall, however, other choices would have been valid as well.

Table 5.3: Value at risk backtest results.

β	s	Level		Smile	
		Long	Short	Long	Short
0.2	1.0%	20.36%	75.06%	100.00%	11.20%
0.2	2.0%	11.20%	34.04%	100.00%	5.65%
0.2	3.0%	11.20%	34.04%	100.00%	5.65%
0.5	1.0%	34.04%	75.06%	100.00%	34.04%
0.5	2.0%	34.04%	75.06%	100.00%	5.65%
0.5	3.0%	20.36%	100.00%	100.00%	5.65%
0.8	1.0%	100.00%	20.36%	100.00%	52.50%
0.8	2.0%	100.00%	75.06%	75.06%	11.20%
0.8	3.0%	34.04%	75.06%	100.00%	5.65%

The p -values from the unconditional coverage backtest from Section 3.3.1.1. The backtests are performed using the level and smile methods from Section 4.2.1 on both the long and the short portfolio with a significance level $\ell = 1\%$.

Table 5.4: Expected shortfall backtest results.

β	s	Level		Smile	
		Long	Short	Long	Short
0.2	1.0%	38.20%	56.00%	24.37%	52.14%
0.2	2.0%	35.11%	68.33%	22.10%	14.51%
0.2	3.0%	32.18%	90.72%	12.97%	12.97%
0.5	1.0%	64.10%	19.98%	16.19%	90.72%
0.5	2.0%	90.72%	29.41%	12.97%	16.19%
0.5	3.0%	64.10%	38.20%	10.27%	24.37%
0.8	1.0%	2.30%	1.22%	12.97%	24.37%
0.8	2.0%	18.01%	8.04%	3.59%	44.86%
0.8	3.0%	41.45%	19.98%	9.10%	18.01%

The p -values from the unconditional coverage backtest from Section 3.3.2.1. The backtests are performed using the level and smile methods from Section 4.2.1 on both the long and the short portfolio with a significance level $\ell = 2.5\%$.

5.3.3 Accuracy of Each Method

In this section, we show the backtest results of each historical simulation method of Chapter 4. For the methods based on Black’s model we use the shift $s_B = 1\%$, and the methods based on the SABR model use the shift $s = 1\%$ and we set $\beta = 0.2$. In Tables 5.5 and 5.6, we show the result from both the unconditional coverage test and the independence test described in Section 3.3.

As in the previous sections, we cannot reject any of the methods based on the results from the unconditional coverage backtest for the value at risk. On the other hand, the results of the independence backtest provide clear evidence to reject the SABR smile model. The reason behind the low p -value in the independence backtest of the SABR smile method will be explained later this section.

Similar to the results of the first backtesting section, the backtests for the expected shortfall are more conclusive. As can be seen, both methods based on Bachelier’s model have p -values below 5% in the unconditional coverage backtest and can thus be rejected. This confirms the findings from Section 5.3.1, that already suggested that the Black’s implied volatility σ_B better captures the market dynamics than the normal implied volatility σ_N from Bachelier’s model. Note that this conclusion can only be drawn from the results of the expected shortfall backtest and not from the backtests of the value at risk. Showing again that a model that is deemed correct for estimating the value at risk, can be rejected when estimating expected shortfall.

Table 5.5: Value at risk backtest results.

Method	Coverage		Independence	
	Long	Short	Long	Short
Black level	75.06%	75.06%	99.04%	98.96%
Black smile	75.06%	75.06%	99.89%	98.96%
Bachelier level	34.04%	34.04%	100.00%	96.17%
Bachelier smile	75.06%	34.04%	98.96%	96.17%
SABR level	20.36%	75.06%	100.00%	22.39%
SABR smile	100.00%	11.20%	99.60%	0.05%

The p -values from the unconditional coverage (left column) and independence (right column) backtests from Sections 3.3.2.1 and 3.3.2.2. The backtests are performed on both the long and the short portfolio with a significance level $\ell = 1\%$.

Table 5.6: Expected shortfall backtest results.

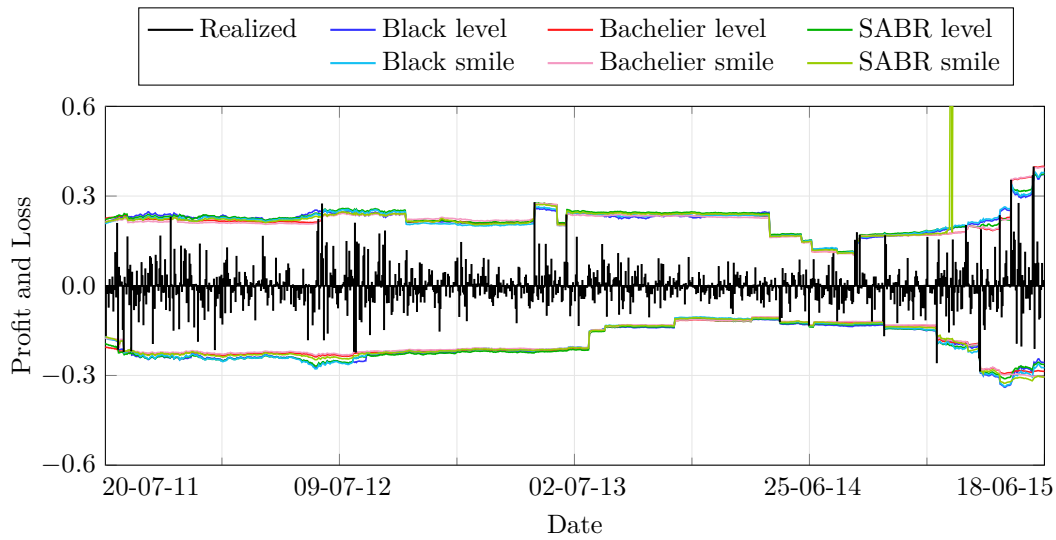
Method	Coverage		Independence	
	Long	Short	Long	Short
Black level	35.11%	10.27%	98.61%	88.84%
Black smile	26.81%	11.56%	97.96%	89.44%
Bachelier level	16.19%	3.10%	99.89%	99.52%
Bachelier smile	3.10%	1.44%	98.47%	99.24%
SABR level	38.20%	56.00%	99.40%	89.95%
SABR smile	24.37%	52.14%	99.90%	69.03%

The p -values from the unconditional coverage (left column) and independence (right column) backtests from Sections 3.3.1.1 and 3.3.1.2. The backtests are performed on both the long and the short portfolio with a significance level $\ell = 2.5\%$.

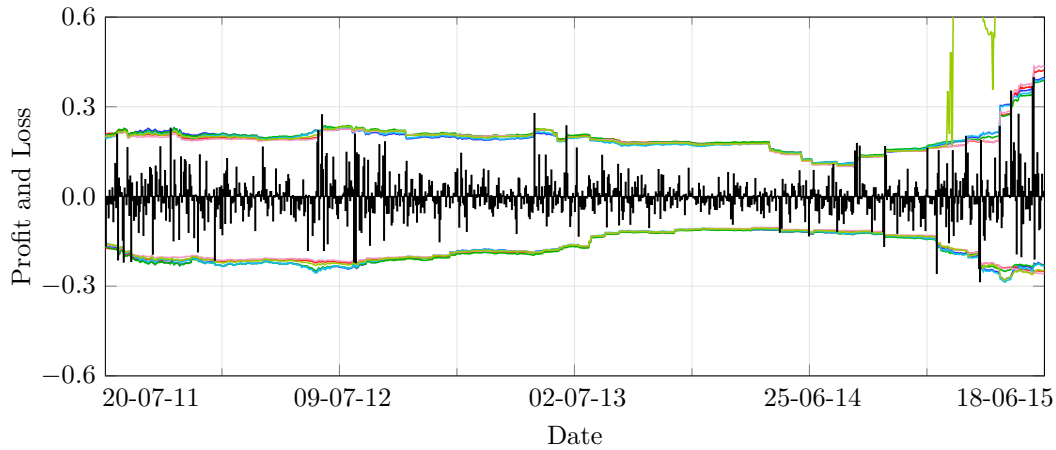
We will also present how the value at risk and expected shortfall estimates line up with the realized profit and loss over time. These results can give additional insights on the accuracy of the different methods and can be found in Figure 5.2.

As can be seen, both the value at risk and expected shortfall estimates from the SABR smile method become unreasonably high at the end of the backtesting period. We observe that these high estimates coincide with a period where the ρ parameter is close to 1 in our market data. In turn, the risk factor $\gamma = \nu\sqrt{1 - \rho^2}$ becomes very small. Since we are using relative shocks for γ , the shocks become very large when γ is small. As a result, some of the scenarios are generated by unreasonable shocks, which causes large losses in the short portfolio that, in turn, produce the high value at risk and expected shortfall estimates. For the value at risk, this resulted in a rejection of the method based on the independence backtest. For the expected

shortfall we would thus expect that the SABR smile method is similarly rejected in the independence backtest. However, this is not the case. One possible reason is that the independence backtest has relatively low power, but more importantly this is a sign that one should not blindly trust the backtesting results and should also analyze the actual estimates of each method.



(a) Time series of the realized profit and loss compared to the value at risk.



(b) Time series of the realized profit and loss compared to the expected shortfall.

Figure 5.2: Time series of the realized profit and loss compared to the value at risk (a) and expected shortfall (b) estimates. The estimates below the realized profit and loss are from the long portfolio whereas the estimates above belong to the short portfolio.

Apart from the problem with the SABR smile method discussed above, we note that all methods produce very similar estimates of both the value at risk and expected shortfall. However, in large portfolios these small differences can become substantial and have a material effect on the capital requirements that are based on these estimates.

Overall, we have found reasons to reject three out of six methods, namely the SABR smile method and both methods based on Bachelier's model. Although we cannot reject the other three methods, this does not necessarily mean that they are correct. However, based on the results of several other backtests using different portfolios, we find some evidence that suggests that the Black smile method is the most robust and gives the most accurate estimates in general. Nevertheless, the methods that only consider changes in the level of the volatility smile give accurate results and it is questionable if incorporating changes in the shape of the volatility smile is worth the extra complexity and effort.

Chapter 6

Conclusion

In this thesis, we investigated the accuracy of historical simulation used to estimate the value at risk and expected shortfall. We focused our research on portfolios consisting of interest rate options. Because some interest rates have recently become negative, this required the development of risk factors that can take this into account. As a second objective, we tested how much the accuracy could be increased by modeling the changes in the shape of the volatility smile as well.

The main contribution of this thesis stems from Theorem 2.28. By adapting the existing SABR formula, we derived a new equation that allows for a change of the shift parameter when computing implied volatilities. This in turn, allows us to compare historical observations of implied volatilities obtained with different shift parameters. This is necessary when we want to use the implied volatility as a risk factor for historical simulation in markets with negative interest rates. Because our solution is based on a closed-form expression, we do not need any numerical methods, resulting in faster and more efficient methods for estimating the value at risk and expected shortfall. Furthermore, by decomposing the SABR formula in a level, slope and curvature component we extended our method such that it can also model changes in the shape of the volatility smile.

Since the Basel Committee on Banking Supervision will require the adoption of the expected shortfall risk measure in the near future, the results of this thesis can provide useful insights. We confirm that historical simulation can be used for the estimation of both the value at risk and expected shortfall, indicating that there is no need for banks to change their methodologies. However, we do find that the accuracy of expected shortfall estimates is more sensitive to the choice of risk factors than the corresponding estimates for the value at risk. Hence, depending on the implementation of the historical simulation method, the adoption of expected shortfall could have an unexpected impact on the regulatory capital.

However, we could not find strong evidence to support that modeling changes in the shape of the volatility smile by additional risk factors can increase the estimation accuracy. This is in line with the findings of Juutilainen (2013) [45], who concludes that including changes of moneyness dependent volatility does not improve the value at risk estimation accuracy. Therefore, it is questionable if incorporating changes in the shape of the volatility smile is worth the extra complexity and modeling effort.

A natural extension of this study would be to use the risk factors derived in this thesis in other historical simulation variants to see if this improves the estimation accuracy. Possibilities include, for example the time-weighted historical simulation by Boudoukh et al. [18], and the filtered historical simulation by Barone-Adesi et al. [17, 21]. Additionally, more extensive backtesting, using a larger backtesting period with more diverse and exotic test portfolios could provide an answer to which risk factors produce the most accurate estimates of the value at risk and expected shortfall.

The main focus of this research has been to investigate which risk factors are applicable to model the volatility smile. An interesting extension of this would be to also focus on different methods to apply historical shocks to the interest rates. To this end, it would be interesting to see if more accurate forecasts are possible when using relative shocks to the shifted interest rates as explained by Fries et al. [43]. This could also lead to a method of estimating the shift parameter in the Black's model based methods of this thesis and lead to an overall more consistent historical simulation framework.

References

- [1] Louis Bachelier. “Théorie de la spéculation”. In: *Annales Scientifiques de l'École Normale Supérieure* 3.17 (1900), pp. 21–86.
- [2] Kenneth Levenberg. “A Method for the Solution of Certain Non-Linear Problems in Least Squares”. In: *Quarterly of Applied Mathematics* 2 (1944), pp. 164–168.
- [3] Donald Marquardt. “An Algorithm for Least-Squares Estimation of Nonlinear Parameters”. In: *SIAM Journal on Applied Mathematics* 11.2 (1963), pp. 431–441.
Available at: <http://www.jstor.org/stable/2098941>.
- [4] Dorian Feldman and Howard G. Tucker. “Estimation of Non-Unique Quantiles”. In: *The Annals of Mathematical Statistics* 37.2 (1966), pp. 451–457.
Available at: <http://www.jstor.org/stable/2238617>.
- [5] George E. P. Box and David A. Pierce. “Distribution of Residual Autocorrelations in Autoregressive-Integrated Moving Average Time Series Models”. In: *Journal of the American Statistical Association* 65.332 (1970), pp. 1509–1526.
Available at: <http://www.jstor.org/stable/2284333>.
- [6] Fischer Black. “The Pricing of Commodity Contracts”. In: *Journal of Financial Economics* 3.1 (1976), pp. 167–179.
Available at: [http://dx.doi.org/10.1016/0304-405X\(76\)90024-6](http://dx.doi.org/10.1016/0304-405X(76)90024-6).
- [7] James A. Koziol and Michael D. Perlman. “Combining Independent Chi-Squared Tests”. In: *Journal of the American Statistical Association* 73.364 (1978), pp. 753–763.
- [8] Greta M. Ljung and George E. P. Box. “On a Measure of a Lack of Fit in Time Series Models”. In: *Biometrika* 65.2 (1978), pp. 297–303.
Available at: <http://www.jstor.org/stable/2284333>.
- [9] J. Michael Harrison and Stanley R. Pliska. “Martingales and Stochastic Integrals in the Theory of Continuous Trading”. In: *Stochastic Processes and their Applications* 11.3 (1981), pp. 215–260.
Available at: [http://dx.doi.org/10.1016/0304-4149\(81\)90026-0](http://dx.doi.org/10.1016/0304-4149(81)90026-0).

- [10] J. Michael Harrison and Stanley R. Pliska. “A Stochastic Calculus Model of Continuous Trading: Complete Markets”. In: *Stochastic Processes and their Applications* 15.3 (1983), pp. 313–316.
Available at: [http://dx.doi.org/10.1016/0304-4149\(83\)90038-8](http://dx.doi.org/10.1016/0304-4149(83)90038-8).
- [11] Charles R. Nelson and Andrew F. Siegel. “Parsimonious Modeling of Yield Curves”. In: *Journal of Business* 60.4 (1987), pp. 473–489.
Available at: <http://www.jstor.org/stable/2352957>.
- [12] Farshid Jamshidian. “An Exact Bond Option Pricing Formula”. In: *The Journal of Finance* 44.1 (1989), pp. 205–209.
Available at: <http://dx.doi.org/10.1111/j.1540-6261.1989.tb02413.x>.
- [13] Lars E. O. Svensson. “Estimating Forward Interest Rates with the Extended Nelson and Siegel Method”. In: *Sveriges Riksbank Quarterly Review* 3 (1995), pp. 13–26.
- [14] Darryll Hendricks. “Evaluation of Value-at-Risk Models Using Historical Data”. In: *Economic Policy Review* 2.1 (1996), pp. 39–69.
Available at: <http://www.ny.frb.org/research/epr/96v02n1/9604hend.html> or <http://dx.doi.org/10.2139/ssrn.1028807>.
- [15] Farshid Jamshidian. “Libor and Swap Market Models and Measures”. In: *Finance and Stochastics* 1.4 (1997), pp. 293–330.
Available at: <http://dx.doi.org/10.1007/s007800050026>.
- [16] Allan M. Malz. “Option-Implied Probability Distributions and Currency Excess Returns”. In: *FEB of New York Staff Report* 32 (1997).
Available at: http://www.newyorkfed.org/research/staff_reports/sr32.html or <http://dx.doi.org/10.2139/ssrn.943500>.
- [17] Giovanni Barone-Adesi, Frederick Bourgoïn, and Kostas Giannopoulos. “Don’t look back”. In: *Risk* 11 (1998), pp. 100–104.
- [18] Jacob Boudoukh, Matthew P. Richardson, and Robert Whitelaw. “The Best of Both Worlds: A Hybrid Approach to Calculating Value at Risk”. 1998.
Available at: <http://dx.doi.org/10.2139/ssrn.51420>.
- [19] Peter F. Christoffersen. “Evaluating Interval Forecasts”. In: *International Economic Review* 39.4 (1998), pp. 841–862.
Available at: <http://www.jstor.org/stable/2527341>.
- [20] Philippe Artzner, Freddy Delbaen, Jean-Marc Eber, and David Heath. “Coherent Measures of Risk”. In: *Mathematical Finance* 9.3 (1999), pp. 203–228.
Available at: <http://dx.doi.org/10.1111/1467-9965.00068>.
- [21] Giovanni Barone-Adesi, Kostas Giannopoulos, and Les Vosper. “VaR Without Correlations for Non-linear Portfolios”. In: *Journal of Futures Markets* 19 (1999), pp. 583–602.
- [22] Allan M. Malz. “Vega Risk and the Smile”. In: *RiskMetrics Working Paper* 99–06 (2000).
Available at: <http://dx.doi.org/10.2139/ssrn.211468>.

- [23] Carlo Acerbi and Dirk Tasche. “Expected Shortfall: A Natural Coherent Alternative to Value at Risk”. In: *Economic Notes* 31.2 (2002), pp. 379–388. Available at: <http://www.bis.org/bcbs/ca/acertasc.pdf> or <http://dx.doi.org/10.1111/1468-0300.00091>.
- [24] Carlo Acerbi and Dirk Tasche. “On the Coherence of Expected Shortfall”. In: *Journal of Banking and Finance* 26 (2002), pp. 1487–1503. Available at: <http://arxiv.org/abs/cond-mat/0104295>.
- [25] Patrick Burns. “Robustness of the Ljung-Box Test and its Rank Equivalent”. 2002. Available at: <http://dx.doi.org/10.2139/ssrn.443560>.
- [26] Hans Föllmer and Alexander Schied. “Convex Measures of Risk and Trading Constraints”. In: *Finance and Stochastics* 6.4 (2002), pp. 429–447. Available at: <http://dx.doi.org/10.1007/s007800200072>.
- [27] Patrick S. Hagan, Deep Kumar, Andrew S. Lesniewski, and Diana E. Woodward. “Managing Smile Risk”. In: *Wilmott magazine* (2002). Available at: <http://www.math.ku.dk/~rolf/SABR.pdf>.
- [28] Henri Berestycki, Jérôme Busca, and Igor Florent. “Computing the Implied Volatility in Stochastic Volatility Models”. In: *Communications on Pure and Applied Mathematics* 57.10 (2004), pp. 1352–1373. Available at: <http://dx.doi.org/10.1002/cpa.20039>.
- [29] Basel Committee on Banking Supervision. *International Convergence of Capital Measurement and Capital Standards*. Tech. rep. Bank for International Settlements, 2005. Available at: <http://www.bis.org/publ/bcbs107.pdf> and <http://www.bis.org/publ/bcbs107b.pdf>.
- [30] Sean D. Campbell. “A Review of Backtesting and Backtesting Procedures”. 2005. Available at: <http://www.federalreserve.gov/pubs/feds/2005/200521/200521pap.pdf>.
- [31] Jón Daniélsson, Bjørn N. Jorgensen, Gennady Samorodnitsky, Mandira Sarma, and Casper G. de Vries. “Subadditivity Re-Examined: The Case for Value-at-Risk”. In: *FMG Discussion Papers* (2005). Available at: <http://eprints.lse.ac.uk/24668/1/dp549.pdf>.
- [32] Alexander J. McNeil, Rüdiger Frey, and Paul Embrechts. *Quantitative Risk Management: Concepts, Techniques, and Tools*. Princeton University Press, 2005.
- [33] Matthias Degen, Paul Embrechts, and Dominik D. Lambrigger. “The Quantitative Modeling of Operational Risk: Between G-and-H and EVT”. In: *The Journal of the International Actuarial Association* 37.2 (2007), pp. 265–291.

- [34] Hans Föllmer and Alexander Schied. “Convex and Coherent Risk Measures”. 2008.
Available at: <http://www.math.hu-berlin.de/~foellmer/papers/CCRM.pdf>.
- [35] Jan Oblój. “Fine-Tune Your Smile”. 2008.
Available at: <http://arxiv.org/abs/0708.0998>.
- [36] Damir Filipović. *Term-Structure Models*. Springer, 2009.
- [37] Leif B. G. Andersen and Vladimir V. Piterbarg. *Interest Rate Modeling. Volume 1: Foundations and Vanilla Models*. Atlantic Financial Press, 2010.
- [38] Christophe Perignon and Daniel R. Smith. “The Level and Quality of Value-at-Risk Disclosure by Commercial Banks”. In: *Journal of Banking and Finance* 32.2 (2010), pp. 362–377.
Available at: <http://dx.doi.org/10.2139/ssrn.952595>.
- [39] Basel Committee on Banking Supervision. *Messages from the Academic Literature on Risk Measurement for the Trading Book*. Tech. rep. Bank for International Settlements, 2011.
Available at: http://www.bis.org/publ/bcbs_wp19.pdf.
- [40] Cyril Grunspan. “A Note on the Equivalence between the Normal and the Lognormal Implied Volatility: A Model Free Approach”. 2011.
Available at: <http://arxiv.org/abs/1112.1782>.
- [41] Claudio Moni. “Risk Managing Long-Dated Smile Risk with SABR Formula”. 2011.
Available at: <http://dx.doi.org/10.2139/ssrn.2349627>.
- [42] Amit Mehta, Max Neukirchen, Sonja Pfetsch, and Thomas Poppensieker. “Managing Market Risk: Today and Tomorrow”. In: *McKinsey Working Papers on Risk* 32 (2012).
- [43] Christian P. Fries, Tobias Nigbur, and Norman Seeger. “Displaced Historical Simulation is a Solution for Negative-Valued Financial Risk Values”. 2013.
Available at: <http://dx.doi.org/10.2139/ssrn.2194917>.
- [44] Keith Head. “Skewed and Extreme: Useful Distributions for Economic Heterogeneity”. 2013.
Available at: <http://strategy.sauder.ubc.ca/head/Papers/skewed.pdf>.
- [45] Ilkka Juutilainen. “From Smile to Smirk: The Relevance of Implied Volatility Skew Changes in Swaption VaR Estimation”. MA thesis. Aalto University, 2013.
- [46] Fabien Le Floc’h and Gary J. Kennedy. “Explicit SABR Calibration Through Simple Expansions”. 2014.
Available at: <http://dx.doi.org/10.2139/ssrn.2467231>.

- [47] Claudio Moni. *Risk Managing Smile Risk with SABR Model*. WBS Interest Rate Conference. 2014.
Available at: <http://ssrn.com/abstract=2527480>.
- [48] Basel Committee on Banking Supervision. *Consultative Document: Fundamental Review of the Trading Book*. Tech. rep. Bank for International Settlements, 2015.
Available at: <http://www.bis.org/publ/bcbs219.pdf>, <http://www.bis.org/publ/bcbs265.pdf> and <http://www.bis.org/bcbs/publ/d305.pdf>.
- [49] Nick Costanzino and Mike Curran. “Backtesting General Spectral Risk Measures with Application to Expected Shortfall”. 2015.
Available at: <http://dx.doi.org/10.2139/ssrn.2514403>.
- [50] Zaichao Du and Juan C. Escanciano. “Backtesting Expected Shortfall: Accounting for Tail Risk”. 2015.
Available at: <http://dx.doi.org/10.2139/ssrn.2548544>.